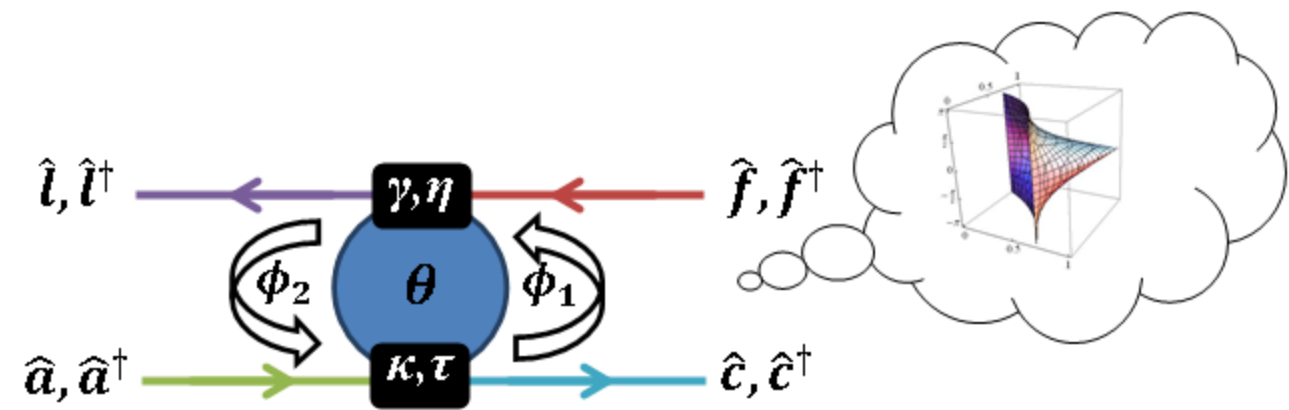


Linear optical quantum information processing in silicon nanophotonics

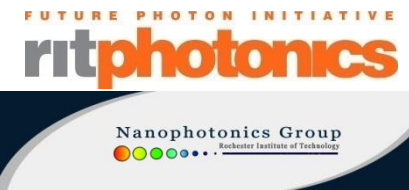


Edwin E. Hach, III
School of Physics and Astronomy
Rochester Institute of Technology



23 Jan 2019

PfQ



I am grateful to pursue the work described here in collaboration with...



Dr. Stefan F. Preble, Microsystems Engineering, RIT



Dr. Ali W. Elshaari, KTH Royal Inst. of Tech., Stockholm



Dr. Paul M. Alsing, Air Force Research Lab, Rome, NY

Michael L. Fanto, Air Force Research Lab, Rome, NY

Dr. A. Matthew Smith, Air Force Research Lab, Rome, NY

Dr. Christopher C. Tison, Air Force Research Lab, Rome, NY

RIT Students:

Jeffrey Steidle*

Ryan Scott**

Thomas Kilmer**

David Spiecker**



**

23 Jan 2019

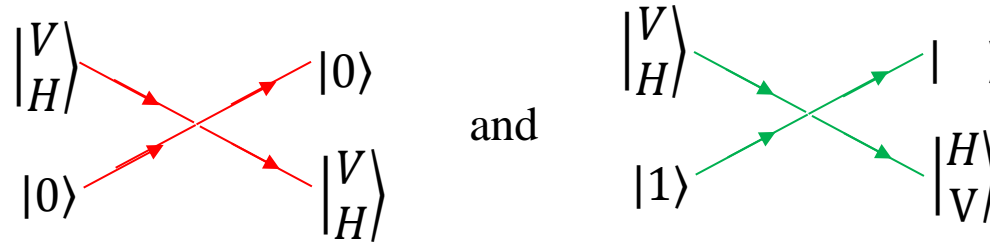


*



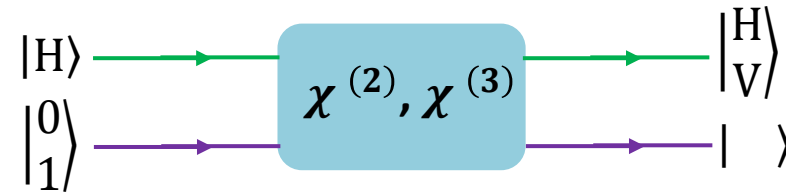
Prologue: Photonic Control of Photons (Deterministic)...

We wish this would happen ...



... but it requires an intensity on the order of 10^{33} W/cm^2

So we search for nonlinear crystals to mediate the interaction...

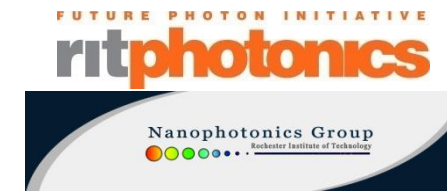


... but media having nonlinear susceptibilities large enough for practical applications are not readily available



23 Jan 2019

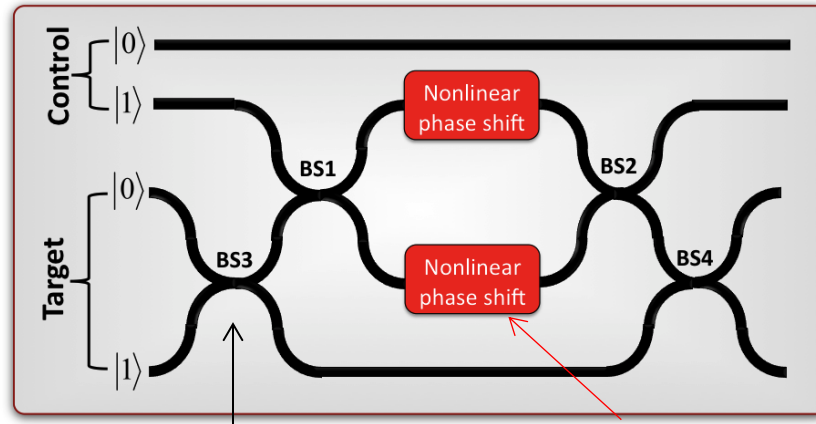
PfQ



Nanophotonics Group
Rochester Institute of Technology

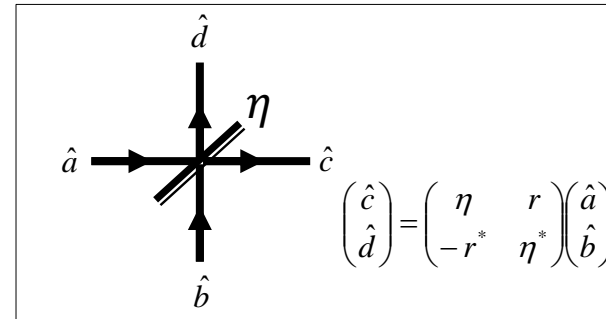
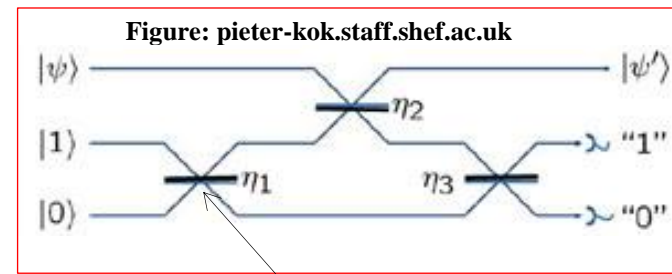
Prologue: Photonic Control of Photons (Probabilistic)...

Linear Optical Quantum Information Processing



Control	Target In	Target Out
0	0	0
0	1	1
1	0	1
1	1	0

Success $\frac{1}{16}$ of the time*



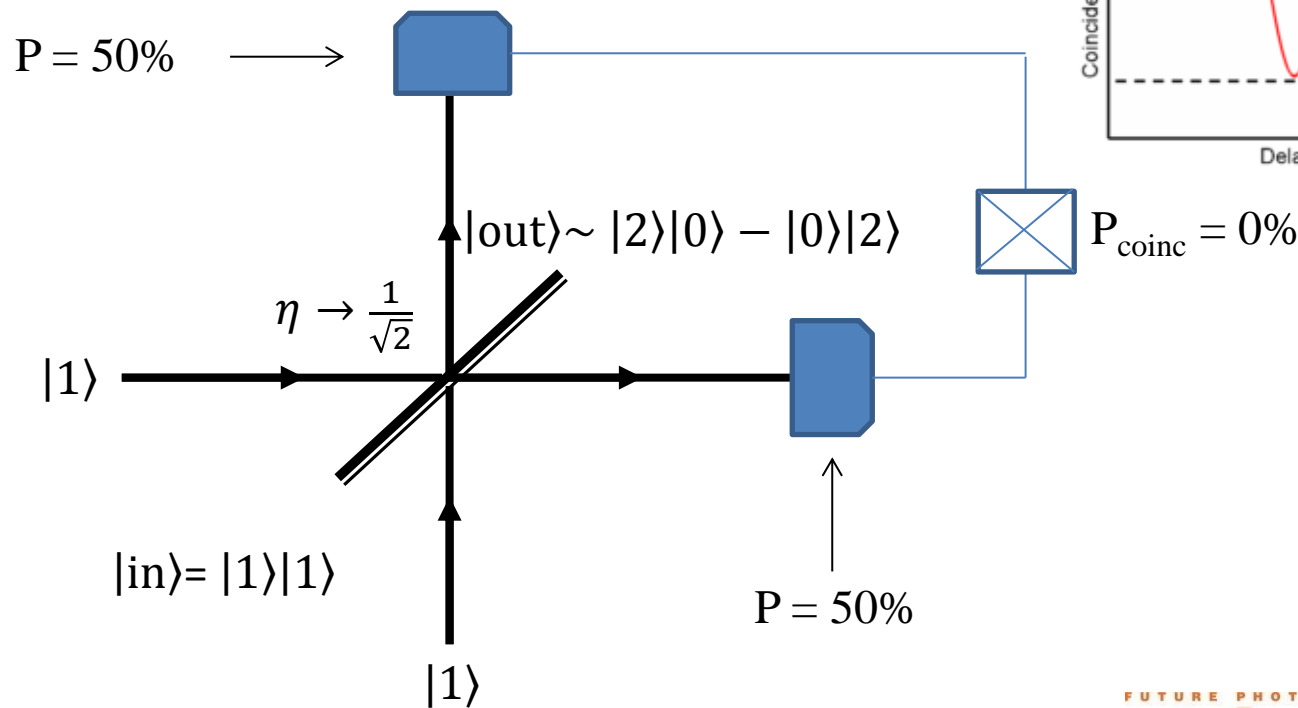
Linear Optical Elements

Desired Characteristics:

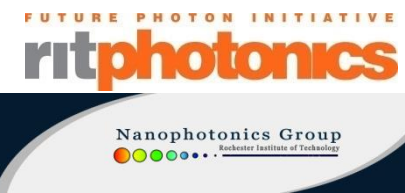
- Scalable
- Dynamically Tunable

Prologue: Photonic Control of Photons (sort of)...

- **50/50 Beam Splitter**
- **The Hong-Ou-Mandel Effect**
- **Post Selection**



14 Sept 2018

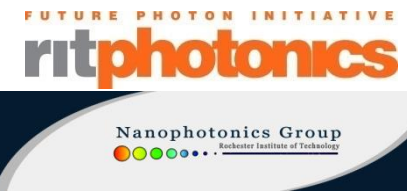


Outline

- **The Goal**
- Input/Output Theory: A General Solution Under Ideal Conditions
- Hong-Ou-Mandel Manifolds: A Promising Result
- Formulation of a Quantum Optical Circuit Theory
- A Scalable KLM CNOT Gate!?
- Engineering and Design: The Fine Print
- Summary and Outlook

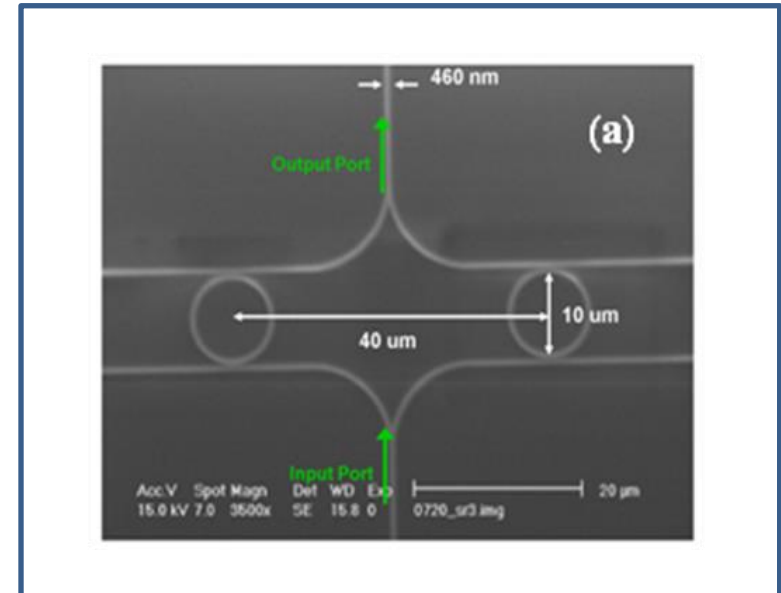
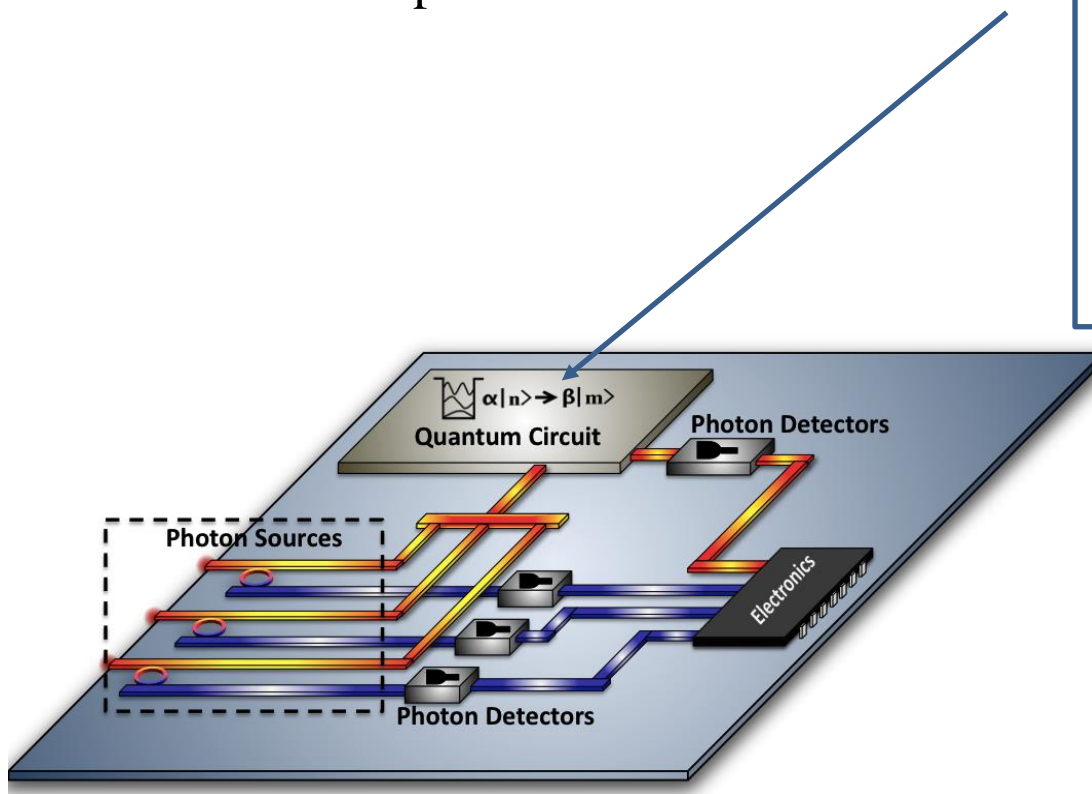


14 Sept 2018



Goal:

Scalable, tunable, on-chip quantum circuits
in silicon nanophotonics ...

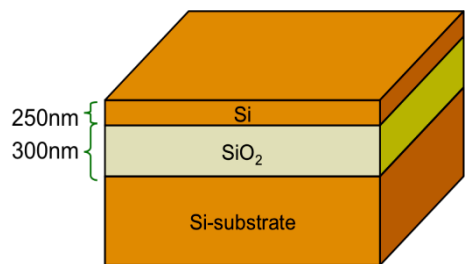


14 Sept 2018

FUTURE PHOTON INITIATIVE
ritphotonics

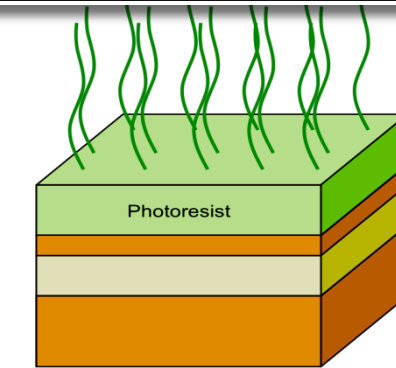
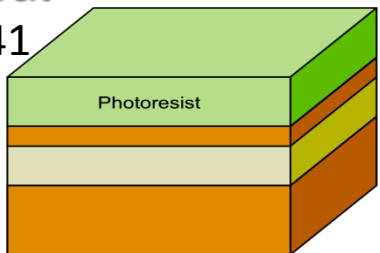


DEVICE FABRICATION I

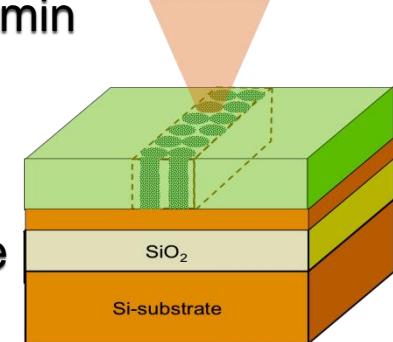


SOI piece

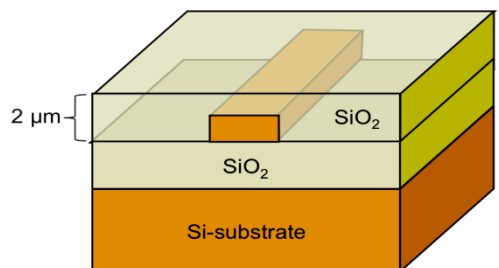
Spin coat
XR-1541



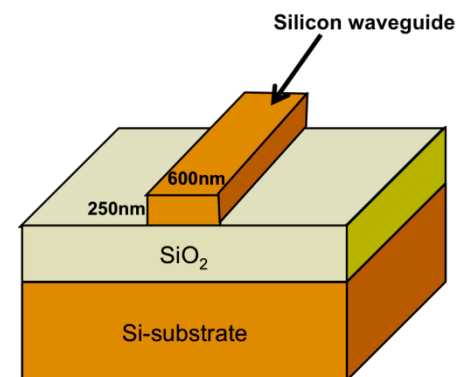
Soft baking
2 min



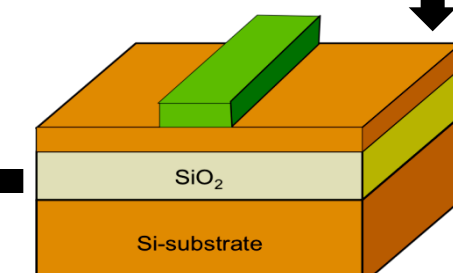
E-beam
exposure



SiO₂ cladding



Si etch (RIE)



Resist developing

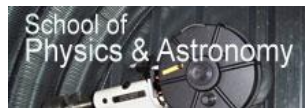
$$\hat{a}_{RIT} \hat{a}_{Cornell}^\dagger | \text{grad students and post docs; no device} \rangle$$

... about 24 hours later ...

$$\hat{a}_{RIT}^\dagger \hat{a}_{Cornell} | \text{grad students and post docs; device} \rangle$$

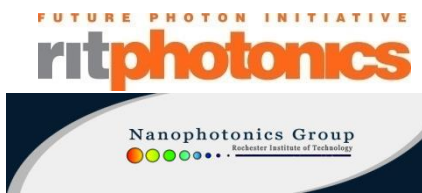
Outline

- The Goal
- Input/Output Theory: A General Solution Under Ideal Conditions
- Hong-Ou-Mandel Manifolds: A Promising Result
- Formulation of a Quantum Optical Circuit Theory
- A Scalable KLM CNOT Gate!?
- Engineering and Design: The Fine Print
- Summary and Outlook



23 Jan 2019

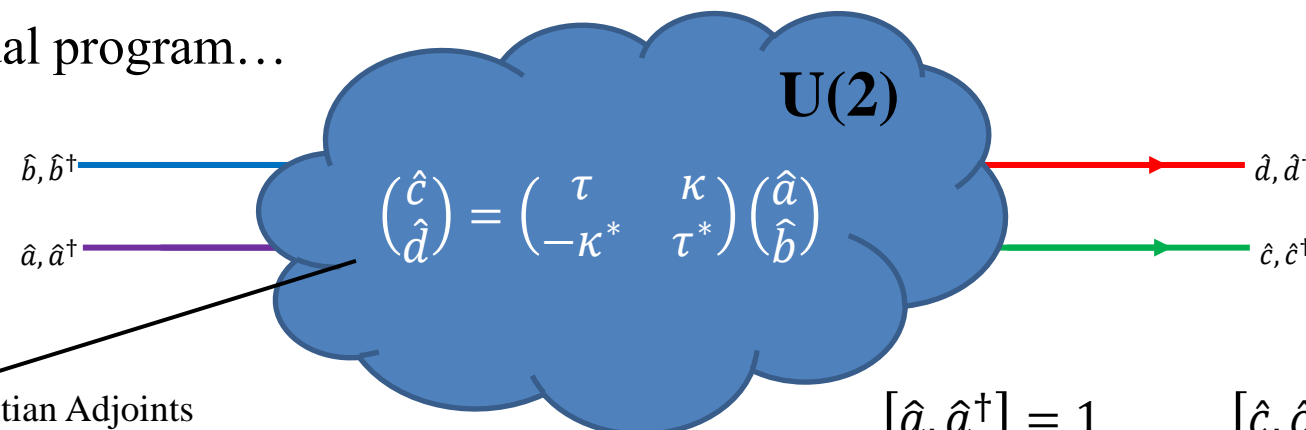
PfQ



10

Linear Quantum Optics on-a-Slide

The usual program...



Invert Hermitian Adjoints

$$\begin{aligned} \hat{a}^\dagger &= \tau \hat{c}^\dagger - \kappa^* \hat{d}^\dagger \\ \hat{b}^\dagger &= \kappa \hat{c}^\dagger + \tau^* \hat{d}^\dagger \end{aligned}$$

$$\begin{aligned} [\hat{a}, \hat{a}^\dagger] &= 1 & [\hat{c}, \hat{c}^\dagger] &= 1 \\ [\hat{b}, \hat{b}^\dagger] &= 1 & [\hat{d}, \hat{d}^\dagger] &= 1 \end{aligned} \Rightarrow$$

$$|\kappa|^2 + |\tau|^2 = 1$$

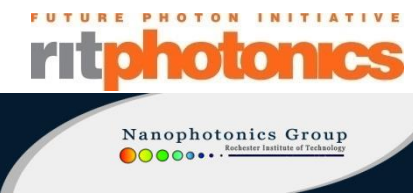
$$|\psi_{\text{in}}\rangle = \sum_{m=0}^{\infty} \sum_{n=0}^{\infty} A_{mn} \frac{(\hat{a}^\dagger)^m (\hat{b}^\dagger)^n}{\sqrt{m! n!}} |\text{vac}\rangle$$

$$\longrightarrow |\psi_{\text{out}}\rangle = \sum_{m=0}^{\infty} \sum_{n=0}^{\infty} \sum_{j=0}^m \sum_{l=0}^n A_{mn} \binom{m}{j} \binom{n}{l} \frac{\tau^j (-\kappa^*)^{m-j} \kappa^l \tau^{*n-l}}{\sqrt{m! n!}} (\hat{c}^\dagger)^{j+l} (\hat{d}^\dagger)^{m+n-j-l} |\text{vac}\rangle$$



23 Jan 2019

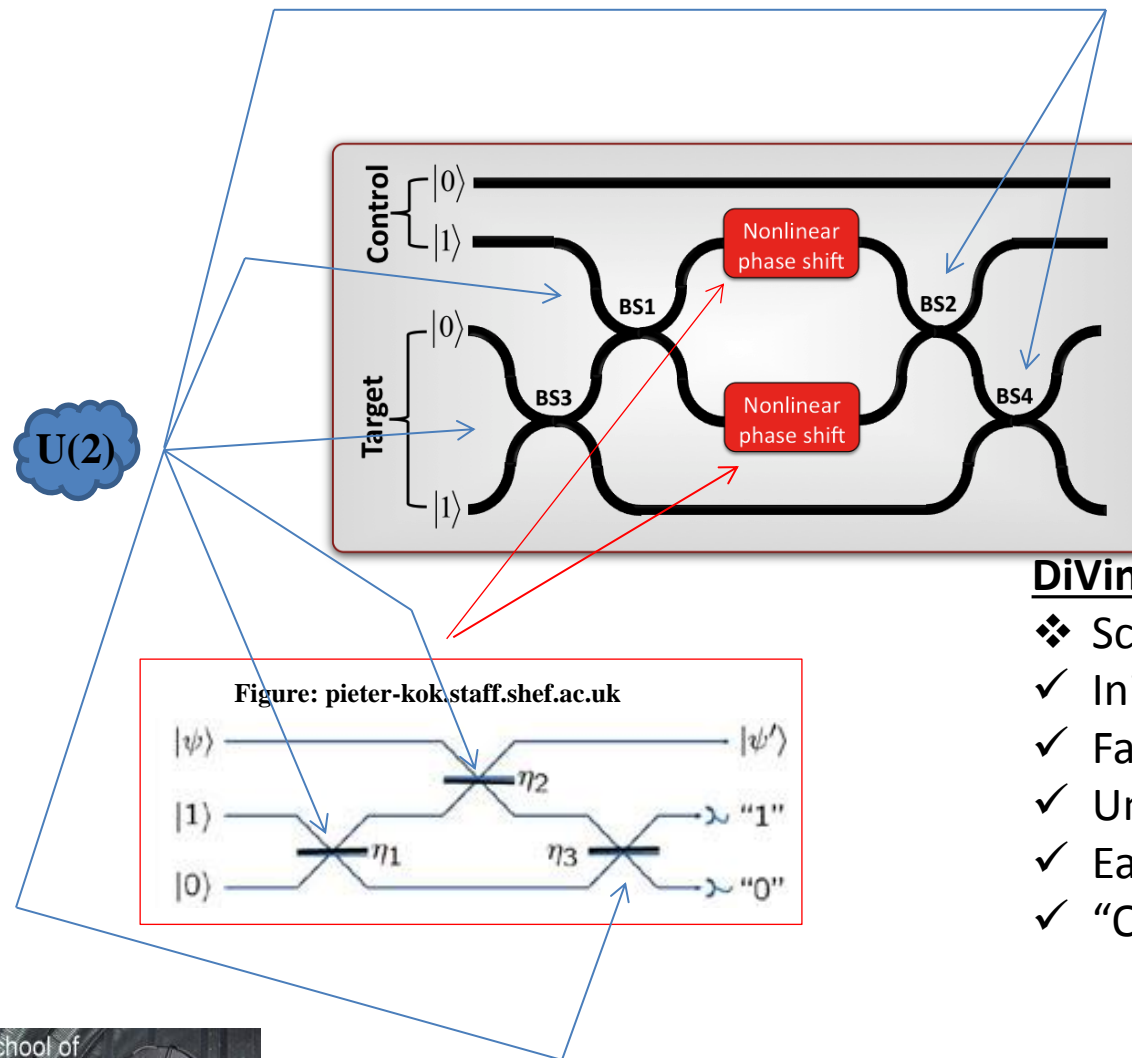
PfQ



Nanophotonics Group
Rochester Institute of Technology

Linear Optical Quantum Information Processing

Knill-Laflamme-Milburn (KLM) Proposal

DiVincenzo Criteria

- ❖ Scalable
- ✓ Initialization of Qubits
- ✓ Faster than Decoherence Time
- ✓ Universal Gates
- ✓ Easy Readout
- ✓ “Quantum” Portability (Qcomm)

FUTURE PHOTON INITIATIVE
ritphotonics



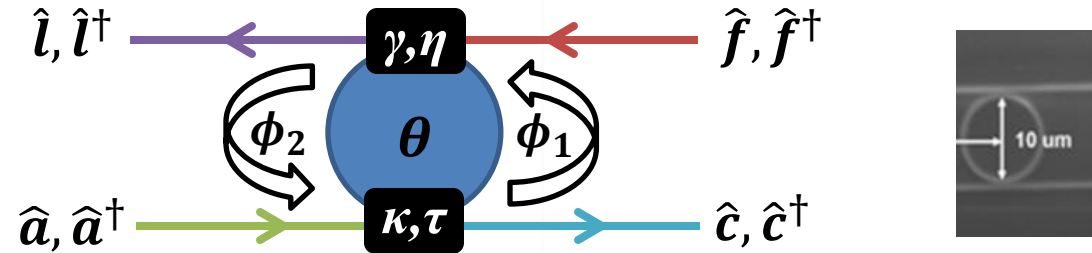
14 Sept 2018



12

To address the problem of scalability for use in an integrated quantum circuit, we consider ...

U(2) Coupled Micro-Ring Resonator (MRR): A Fundamental Circuit Element for Quantum Optics on-a-Chip



Simple Model:

- Continuous Wave (CW) Operation
- “Internal” Modes not Pictured
- Lossless (Unitary) Operation

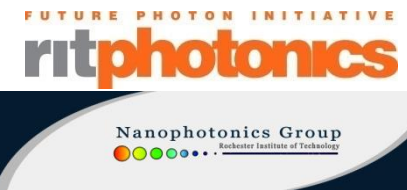
Practical Advantages:

- Scalable
- Can be tuned dynamically
- Stefan et al can make them (they do it all the time)

$$\begin{aligned} [\hat{a}, \hat{a}^\dagger] &= 1 & [\hat{c}, \hat{c}^\dagger] &= 1 \\ [\hat{f}, \hat{f}^\dagger] &= 1 & [\hat{l}, \hat{l}^\dagger] &= 1 \end{aligned} \Rightarrow$$



14 Sept 2018

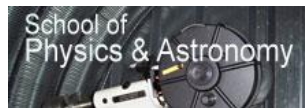


Nanophotonics Group
Rochester Institute of Technology

13

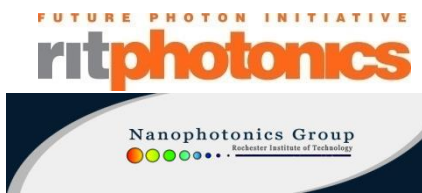
Outline

- The Goal
- **Input/Output Theory: A General Solution Under Ideal Conditions**
- Hong-Ou-Mandel Manifolds: A Promising Result
- Formulation of a Quantum Optical Circuit Theory
- A Scalable KLM CNOT Gate!?
- Engineering and Design: The Fine Print
- Summary and Outlook



23 Jan 2019

PfQ



14

Transition Amplitudes, Quantum Interference, and Path Integrals

The **transition amplitude** for a system to evolve from some initial state to some final state **along a particular path** connecting the initial and final states is a product of transition amplitudes for taking each individual “step” along the path

$$\varphi_{f,i} = \varphi_{f,f-1} \cdot \varphi_{f-1,f-2} \cdots \varphi_{i+2,i+1} \cdot \varphi_{i+1,i}$$

The **transition amplitude** for a system to evolve from some initial state to some final state is determined by the **quantum interference** between transition amplitudes **along all possible paths connecting the initial and final states**

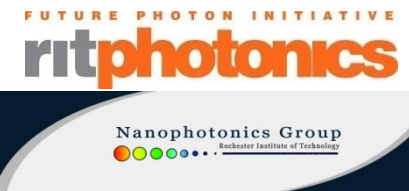
$$\Phi_{i \rightarrow f} = \sum_{\substack{\text{all} \\ \text{paths}}} \varphi_{f,i} \quad (\text{Propagator})$$

The **transition amplitude** for a system to evolve from some initial state to some final state is determined by the **quantum interference** between transition amplitudes **along all possible paths connecting the initial and final states**

$$|f\rangle = \sum_i [\Phi_{i \rightarrow f}] |i\rangle$$



23 Jan 2019



“Discrete Path Integral*” Approach to Linear Quantum Optics

To adapt the Feynman prescription for use in linear quantum optics ...

- 1) Imagine that the Boson operators represent** photons and that photons are little, classical, localized balls of light***
- 2) Enumerate the classical paths of the ‘Boson operators’ through the optical system
- 3) Construct the transition element along each path by multiplying the appropriate transition element for each step (phase shift, reflection, transmission, etc.) along the path
- 4) **Propagator:** sum over all paths connecting particular pairs of input and output modes
- 5) Use the propagator to express each output ‘Boson operator’ as a linear superposition of the inputs
- 6) Forget Step 1 and treat the ‘Boson operators’ like Boson operators

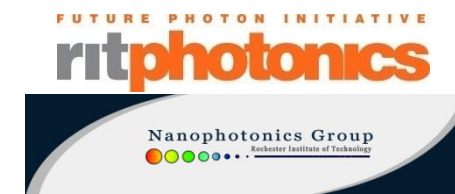
* Skaar et al, and some others, thought of this, too

** They don’t

*** They aren’t



23 Jan 2019



Nanophotonics Group
Rochester Institute of Technology

Phase Shifter U(1)

(rectilinear propagation through linear optical medium)



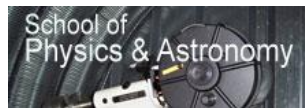
$$\theta = n \frac{\omega L}{c} = \omega t_{\text{int}}$$

$$\hat{a}_{\text{in}} \rightarrow \hat{a}_{\text{out}} = e^{i\theta \hat{a}_{\text{in}}^\dagger \hat{a}_{\text{in}}} \hat{a}_{\text{in}} e^{-i\theta \hat{a}_{\text{in}}^\dagger \hat{a}_{\text{in}}} = \hat{a}_{\text{in}} e^{-i\theta}$$

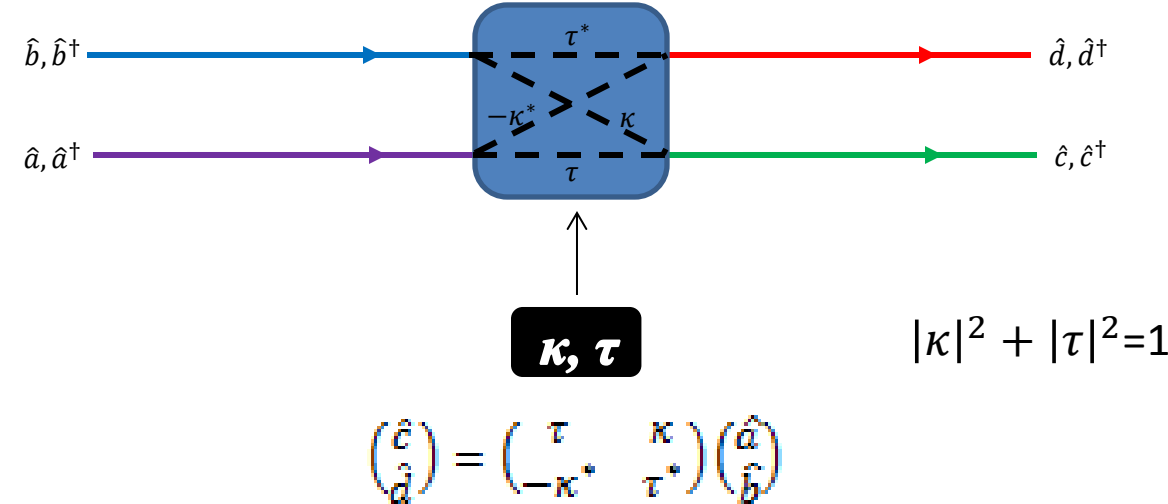
Path	Transition Amplitude
$\hat{a}_{\text{in}} \rightarrow \hat{a}_{\text{out}}$	$e^{-i\theta}$

Linear Quantum Optics: discrete “stepwise” transition amplitudes are generally easy to determine using the Heisenberg Picture

Feynman’s Spacetime Formulation: infinitesimal transition amplitudes are determined using the classical action



Directional Coupler (or any SU(2))

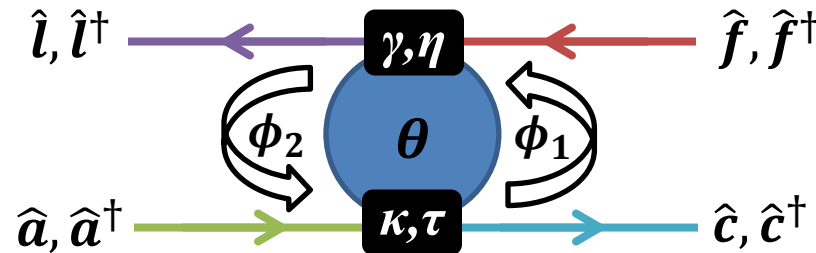


Path (input mode → output mode)	Transition Amplitude Along Path
a → c	τ
a → d	$-\kappa^*$
b → c	κ
b → d	τ^*

Heisenberg Picture: Rotations generated by

$$\hat{J}_1 = \frac{1}{2}(\hat{a}^\dagger \hat{b} + \hat{a} \hat{b}^\dagger) \quad \text{and} \quad \hat{J}_2 = \frac{1}{2i}(\hat{a}^\dagger \hat{b} - \hat{a} \hat{b}^\dagger)$$

Discrete Path Integral (DPI) Formulation of the Basic Ring Resonator Quantum Circuit Element: CW Operation



Path	#Round Trips	Transition Amplitude Along Path
$a \rightarrow c$	0	τ
	1	$(-\kappa^*)(e^{-i\phi_1})(\eta^*)(e^{-i\phi_2})(\kappa)$
	2	$(-\kappa^*)(e^{-i\phi_1})(\eta^*)(e^{-i\phi_2})(\tau^*)(e^{-i\phi_1})(\eta^*)(e^{-i\phi_2})(\kappa)$
	\vdots	\vdots
	n	$(-\kappa^*)(e^{-i\phi_1})(\eta^*)[(\tau^*)(e^{-i\phi_1})(\eta^*)(e^{-i\phi_2})]^{n-1}(\kappa)$
$f \rightarrow c$	"1/2"	$(-\gamma^*)(e^{-i\phi_2})(\kappa)$
	"3/2"	$(-\gamma^*)(e^{-i\phi_2})(\tau^*)(e^{-i\phi_1})(\eta^*)(e^{-i\phi_2})(\kappa)$
	\vdots	\vdots
	$n + "1/2"$	$(-\gamma^*)(e^{-i\phi_2})[(\tau^*)(e^{-i\phi_1})(\eta^*)(e^{-i\phi_2})]^n(\kappa)$
$a \rightarrow l$	"1/2"	$(-\kappa^*)(e^{-i\phi_1})(\gamma)$
	"3/2"	$(-\kappa^*)(e^{-i\phi_1})(\eta^*)(e^{-i\phi_2})(\tau^*)(e^{-i\phi_1})(\gamma)$
	\vdots	\vdots
	$n + "1/2"$	$(-\kappa^*)(e^{-i\phi_1})[(\eta^*)(e^{-i\phi_2})(\tau^*)(e^{-i\phi_1})]^n(\gamma)$
$f \rightarrow l$	0	η
	1	$(-\gamma^*)(e^{-i\phi_2})(\tau^*)(e^{-i\phi_1})(\gamma)$
	2	$(-\gamma^*)(e^{-i\phi_2})(\tau^*)(e^{-i\phi_1})(\eta^*)(e^{-i\phi_2})(\tau^*)(e^{-i\phi_1})(\gamma)$
	\vdots	\vdots
	n	$(-\gamma^*)(e^{-i\phi_2})(\tau^*)(e^{-i\phi_1})[(\eta^*)(e^{-i\phi_2})(\tau^*)(e^{-i\phi_1})]^{n-1}(\gamma)$

$$\hat{c} = [\text{sum over paths in class } a \rightarrow c] \hat{a} + [\text{sum over paths in class } f \rightarrow c] \hat{f}$$

Similar idea for $(a,f) \rightarrow l$



DPI Solution for CW Quantum Transfer Function for Basic Ring Resonator Quantum Circuit Element

$$\hat{c} = [\text{sum over paths in class } a \rightarrow c] \hat{a} + [\text{sum over paths in class } f \rightarrow c] \hat{f}$$

$$= \left[\tau + (-\kappa^*)(\eta^*)(\kappa)(e^{-i\theta}) \sum_{m=0}^{\infty} (\eta^* \tau^* e^{-i\theta})^m \right] \hat{a} + \left[(-\gamma^*)(e^{-i\phi_2})(\kappa) \sum_{m=0}^{\infty} (\eta^* \tau^* e^{-i\theta})^m \right] \hat{f}$$

$$= \left(\tau - \frac{\eta^* |\kappa|^2 e^{-i\theta}}{1 - \eta^* \tau^* e^{-i\theta}} \right) \hat{a} - \left(\frac{\gamma^* \kappa e^{-i\phi_2}}{1 - \eta^* \tau^* e^{-i\theta}} \right) \hat{f}$$

$$\hat{l} = - \left(\frac{\gamma \kappa^* e^{-i\phi_1}}{1 - \eta^* \tau^* e^{-i\theta}} \right) \hat{a} + \left[\eta - \left(\frac{\tau^* |\gamma|^2 e^{-i\theta}}{1 - \eta^* \tau^* e^{-i\theta}} \right) \right] \hat{f}$$

$$\begin{aligned} \hat{a}^\dagger &= t \hat{c}^\dagger + s \hat{l}^\dagger \\ \Rightarrow \hat{f}^\dagger &= s' \hat{c}^\dagger + t' \hat{l}^\dagger \end{aligned}$$

$$t \equiv \left(\frac{\eta^* - \tau e^{i\theta}}{\eta^* \tau^* - e^{i\theta}} \right)$$

$$s \equiv \left(\frac{\gamma \kappa^* e^{i\phi_2}}{\eta^* \tau^* - e^{i\theta}} \right)$$

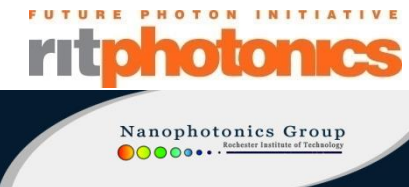
$$s' \equiv \left(\frac{\kappa \gamma^* e^{i\phi_1}}{\eta^* \tau^* - e^{i\theta}} \right)$$

$$t' \equiv \left(\frac{\tau^* - \eta e^{i\theta}}{\eta^* \tau^* - e^{i\theta}} \right)$$

PfQ



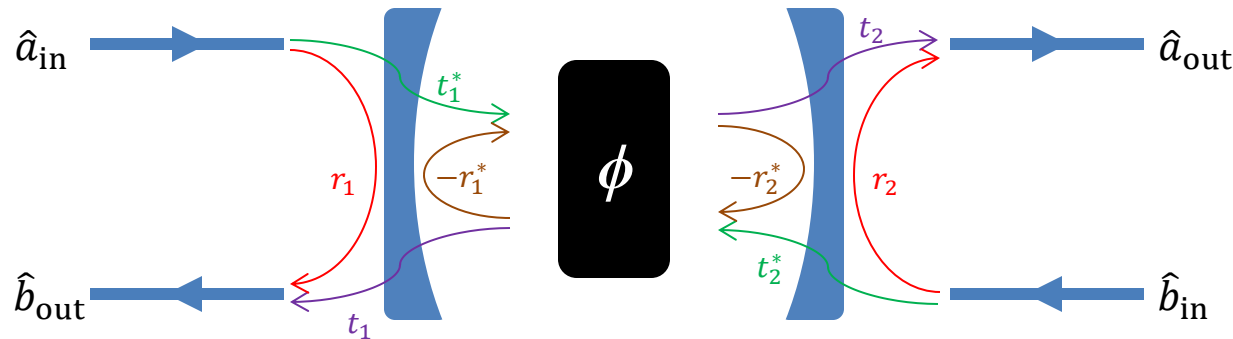
23 Jan 2019



Nanophotonics Group
Rochester Institute of Technology

20

Ring Resonator/Fabry-Perot Etalon Equivalence

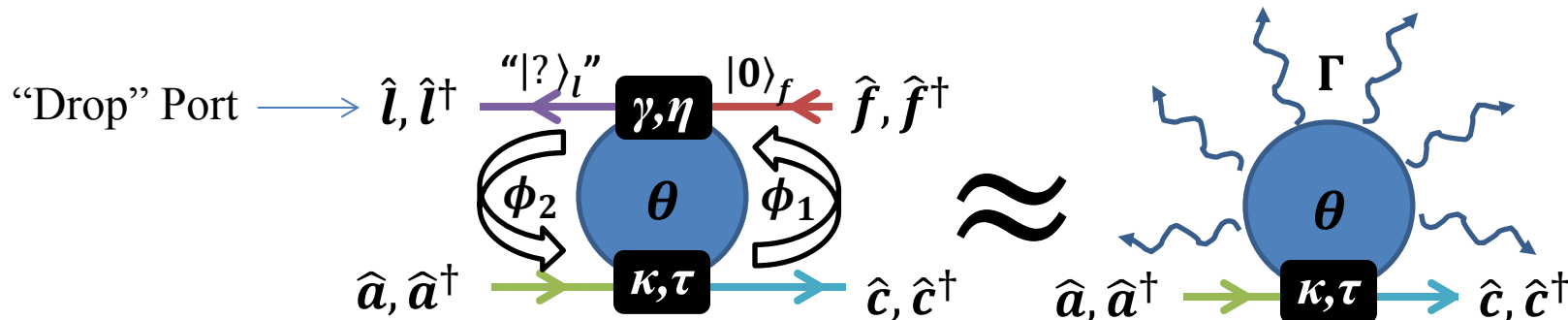


A schematic representation of an externally driven Fabry-Perot etalon. Each distinct input/output optical mode is labeled with its Bosonic annihilation operator. The phase conventions for the transmission and reflection amplitudes adopted here are valid parameterizations for the SU(2) transformations that occur at the lossless, partially reflective mirrors forming the cavity; to facilitate our comparison this is in agreement with the notation in Ref. [8]. The linear phase shift, ϕ , is the phase shift for a single crossing of the cavity; that is, a round trip through the cavity is accompanied by a phase shift of $\theta = 2\phi$.

$$\begin{aligned}\hat{a}_{\text{out}} &= \left(\frac{t_1^* t_2 e^{-i\phi}}{1 - r_1^* r_2^* e^{-2i\phi}} \right) \hat{a}_{\text{in}} + \left(r_2 - \frac{r_1^* |t_2|^2 e^{-2i\phi}}{1 - r_1^* r_2^* e^{-2i\phi}} \right) \hat{b}_{\text{in}} \\ \hat{b}_{\text{out}} &= \left(r_1 - \frac{r_2^* |t_1|^2 e^{-2i\phi}}{1 - r_1^* r_2^* e^{-2i\phi}} \right) \hat{a}_{\text{in}} + \left(\frac{t_1 t_2^* e^{-i\phi}}{1 - r_1^* r_2^* e^{-2i\phi}} \right) \hat{b}_{\text{in}}\end{aligned}$$



R·I·T Simple Model for a Lossy Ring Coupled to a Single Waveguide



1) Solve the deterministic problem:

$$|\psi_{\text{out}}\rangle = (t\hat{c}^\dagger + s\hat{l}^\dagger)|\emptyset\rangle = t|1\rangle_c \otimes |0\rangle_l + s|0\rangle_c \otimes |1\rangle_l \equiv t|1,0\rangle + s|0,1\rangle$$

2) Express the deterministic solution using (pure state) global **density operator**:

$$\hat{\rho}_{\text{out}}^{(G)} = |\psi_{\text{out}}\rangle\langle\psi_{\text{out}}| = |t|^2|1,0\rangle\langle 1,0| + ts^*|1,0\rangle\langle 0,1| + st^*|0,1\rangle\langle 1,0| + |s|^2|0,1\rangle\langle 0,1|$$

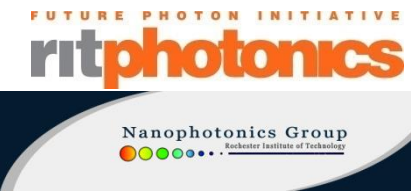
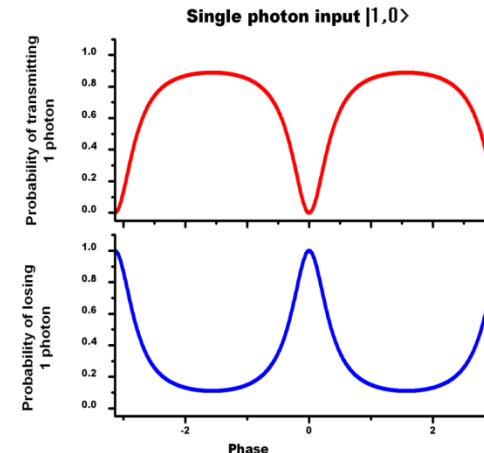
3) Trace over loss channel to obtain (mixed state) reduced density operator for transmission mode:

$$\hat{\rho}_{\text{out}}^{(c)} = \text{Tr}_{\text{mode } l}\{\hat{\rho}_{\text{out}}^{(G)}\} = |t|^2|1\rangle\langle 1| + |s|^2|0\rangle\langle 0|$$

$$P(0,1|1,0) = \frac{|\gamma|^2|\kappa|^2}{1 + |\eta|^2|\tau|^2 - 2\text{Re}[\eta\tau e^{i\theta}]}$$



14 Sept 2018



Comparison with Classical Electrodynamics (Sanity Check)

Parametric Limit

Highly excited ordinary coherent state input along mode a : $\hat{a}|\alpha\rangle = \alpha|\alpha\rangle$

$$|\psi_{\text{in}}\rangle = |\alpha, 0\rangle = \hat{\mathcal{D}}^{(a)}(\alpha) \otimes \hat{\mathbb{I}}^{(f)}|\text{vac}\rangle = \exp(\alpha\hat{a}^\dagger - \alpha^*\hat{a})|\text{vac}\rangle$$

The output (pure state) is a direct product of ordinary coherent states:

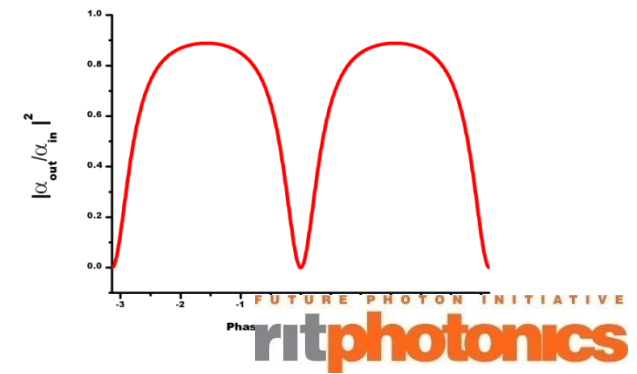
$$|\psi_{\text{out}}\rangle = \hat{\mathcal{D}}^{(c)}(t\alpha) \otimes \hat{\mathcal{D}}^{(l)}(s\alpha)|\text{vac}\rangle = |t\alpha\rangle_c \otimes |s\alpha\rangle_l$$

Specifically, in mode c $\hat{\rho}_{\text{out}}^{(c)} = |t\alpha\rangle\langle t\alpha|$ where $\alpha_{\text{out}} = t\alpha = \left(\frac{\eta^* - \tau e^{i\theta}}{\eta^* \tau^* - e^{i\theta}}\right) \alpha_{\text{in}}$

Quantity	Yariv Treatment	Classical Factor	Fully QM Treatment w/ Coherent State
Input Field Amplitude	"Circulation Method"	1	α_{in}
Output Field Amplitude (waveguide)		b_1	α_{out}
"CirculationFactor"/Internal Transmission Amplitude at Drop Port		α	η^*
Round Trip Phase		θ	$-\theta$
$a \rightarrow c$ transition Amplitude		t	τ



A. Yariv, *Electronics Letters* **36**, 321 (2000)



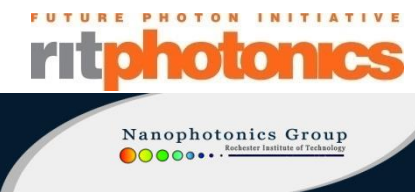
Outline

- The Goal
- Input/Output Theory: A General Solution Under Ideal Conditions
- **Hong-Ou-Mandel Manifolds: A Promising Result**
- Formulation of a Quantum Optical Circuit Theory
- A Scalable KLM CNOT Gate!?
- Engineering and Design: The Fine Print
- Summary and Outlook



23 Jan 2019

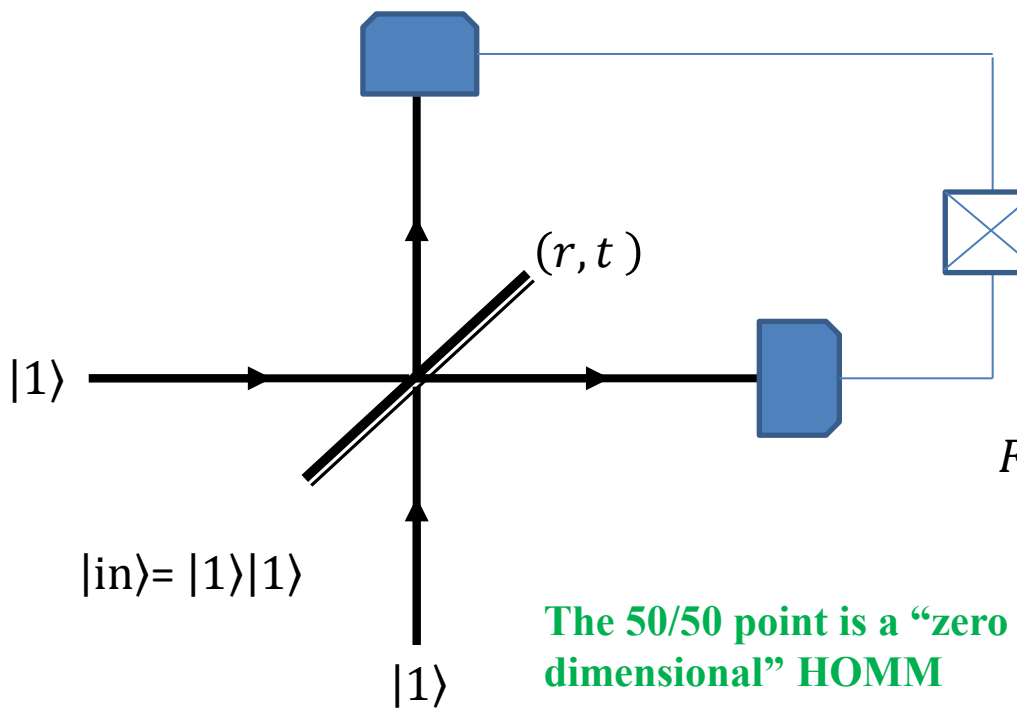
PfQ



24

Hong-Ou-Mandel Effect (Beam Splitter/Bulk Optics)

At the 50/50 operating **point**: $|1,1\rangle \rightarrow |2 :: 0\rangle = \frac{1}{\sqrt{2}}(|2,0\rangle - |0,2\rangle)$

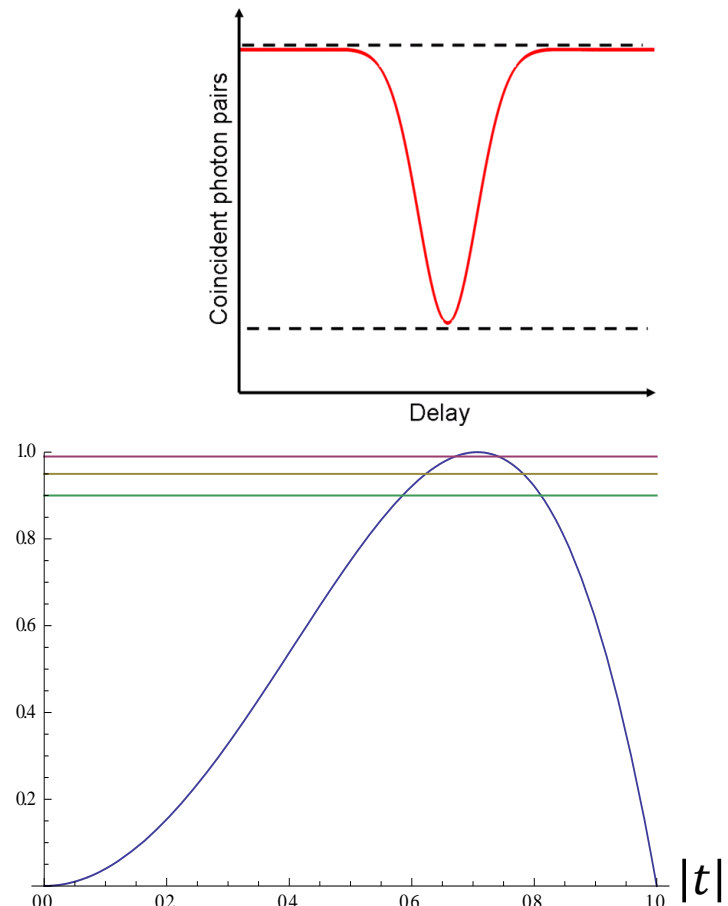


H-O-M Output State Fidelity:

$$F \equiv |\langle 2 :: 0 | \text{out} \rangle|^2$$

$$0 \leq F \leq 1$$

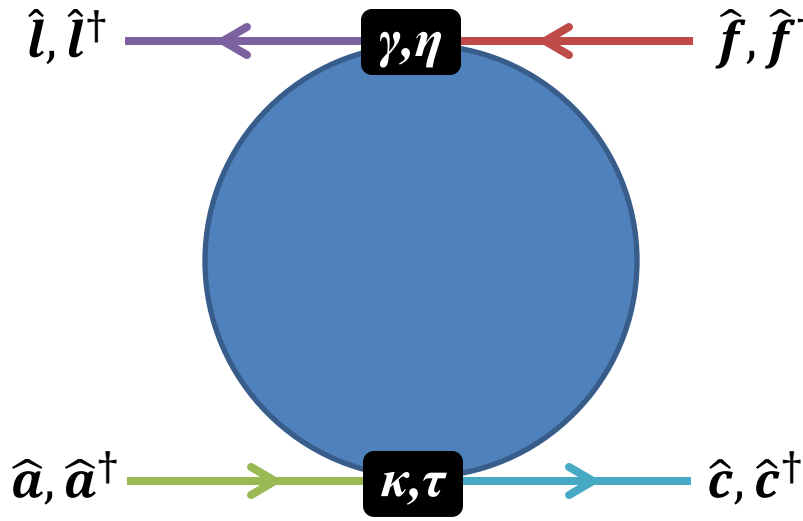
HOM 2-photon interference



FUTURE PHOTON INITIATIVE
ritphotonics



Two Photon Driving: Hong-Ou-Mandel Manifolds (HOMM)



$$t \equiv \left(\frac{\eta^* - \tau e^{i\theta}}{\eta^* \tau^* - e^{i\theta}} \right)$$

$$s \equiv \left(\frac{\gamma \kappa^* e^{i\phi_2}}{\eta^* \tau^* - e^{i\theta}} \right)$$

$$t' \equiv \left(\frac{\tau^* - \eta e^{i\theta}}{\eta^* \tau^* - e^{i\theta}} \right)$$

$$s' \equiv \left(\frac{\kappa \gamma^* e^{i\phi_1}}{\eta^* \tau^* - e^{i\theta}} \right)$$

Input state: $|\psi_{\text{in}}\rangle = |1,1\rangle = \hat{a}^\dagger \hat{f}^\dagger |\emptyset\rangle$

Output state: $|\psi_{\text{out}}\rangle = \sqrt{2}ts' |2,0\rangle + (tt' + ss') |1,1\rangle + \sqrt{2}st' |0,2\rangle$

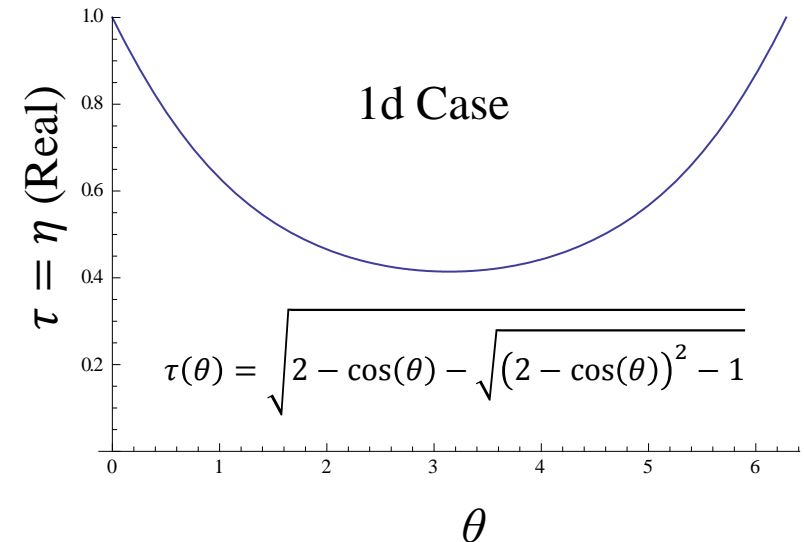
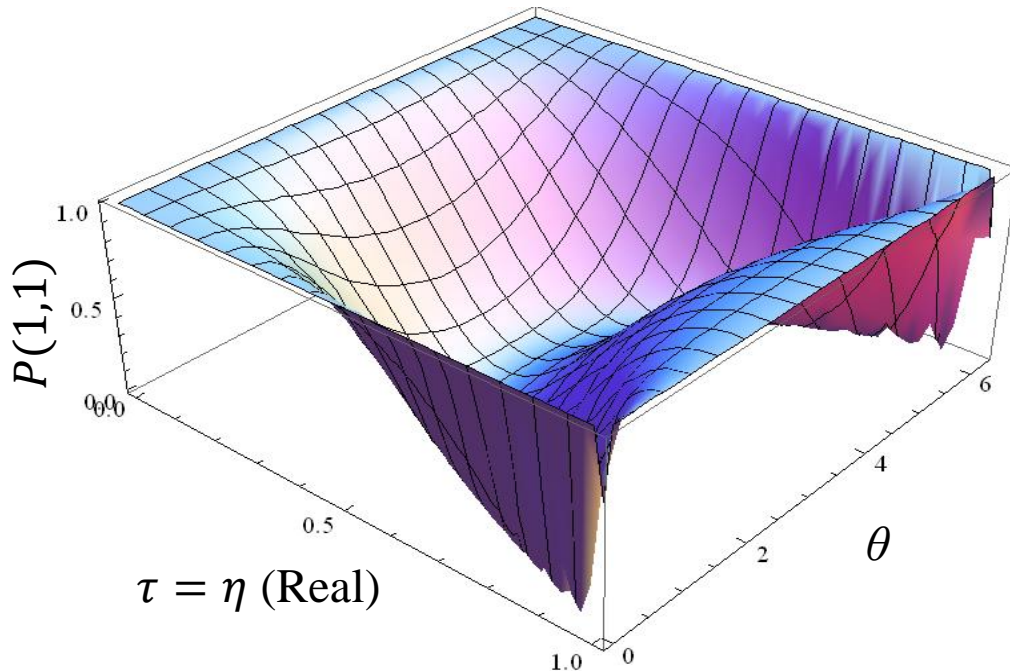
HOMM: $tt' + ss' = 0 \Rightarrow |\kappa|^2 + |\gamma|^2 + |\kappa|^2 |\gamma|^2 + 2\text{Re}(\eta \tau e^{i\theta}) = 2$



23 Jan 2019

Hong-Ou-Mandel Manifolds: Robust Two-Photon “Bunching”

$$\text{HOMM: } tt' + ss' = \mathbf{0} \rightarrow |\kappa|^2 + |\gamma|^2 + |\kappa|^2|\gamma|^2 + 2\text{Re}(\eta\tau e^{i\theta}) = 2$$



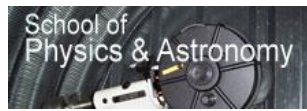
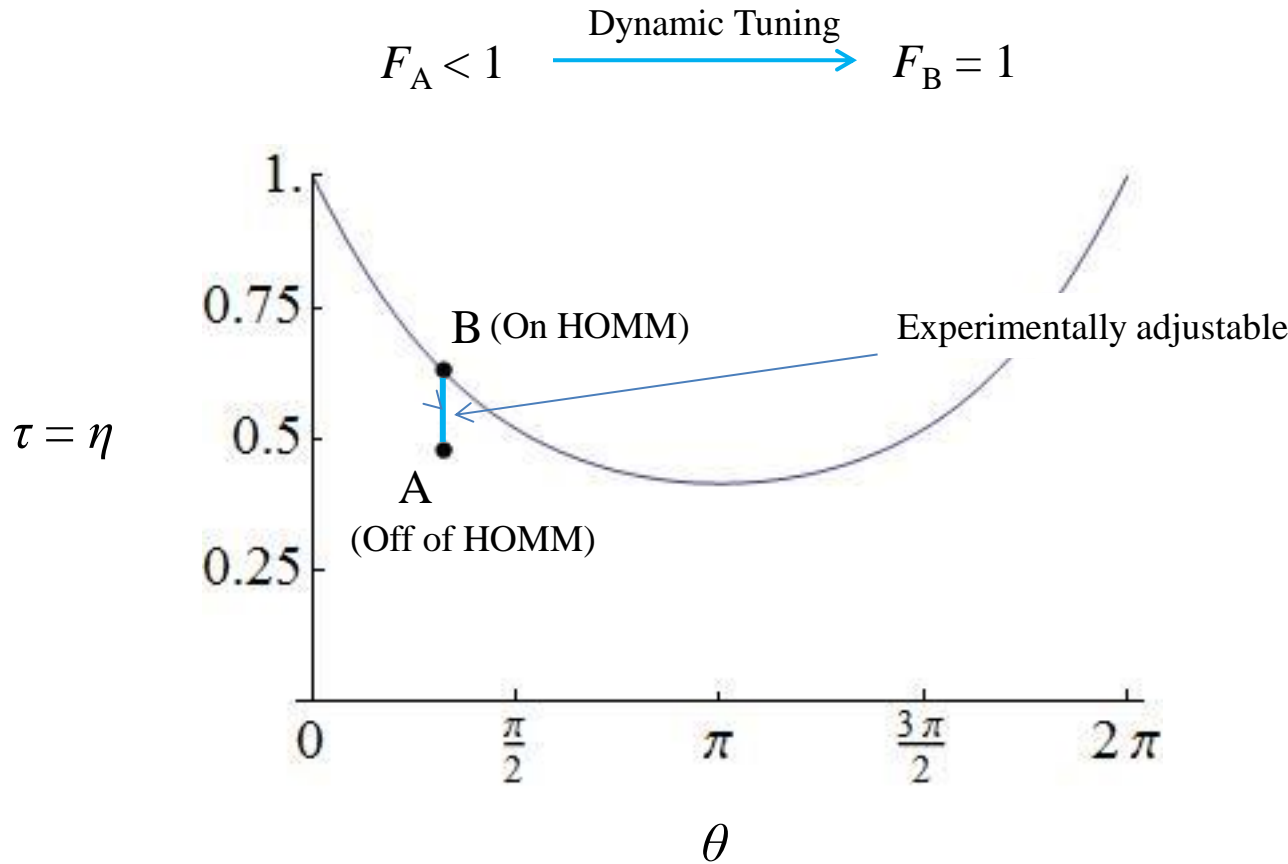
Parameter space of ring resonator circuit element features a differentiable manifold of operating points on which the HOM Effect occurs ... this will translate into enhanced robustness in the operation of devices that rely on this effect.

EEHIII, S.F. Preble, A.W. Elshaari, P.M. Alsing and M.L. Fanto, *Phys. Rev. A***89**, 043805 (2014)



23 Jan 2019

Hong-Ou-Mandel Manifolds Allow for Operational Optimization of a Scalable U(2) Device

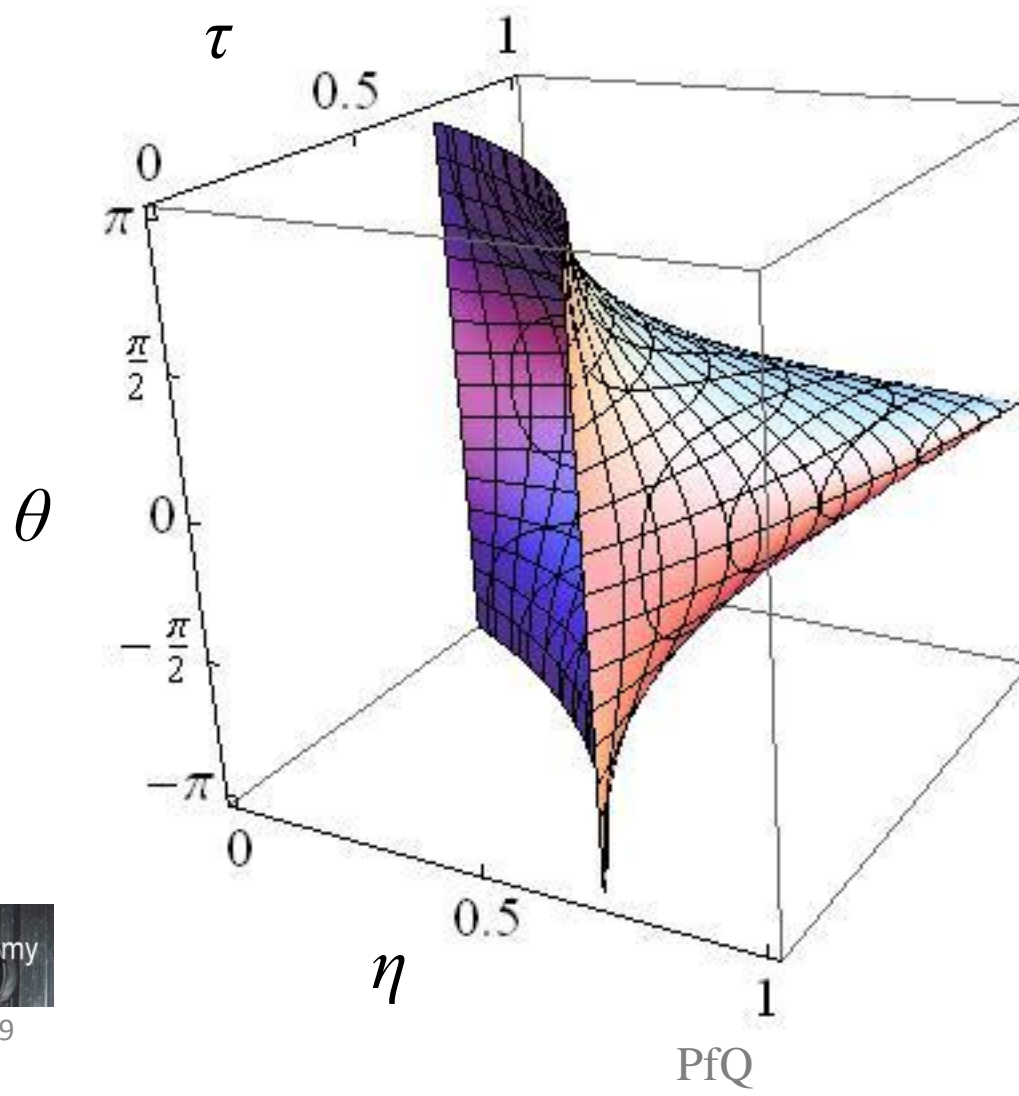


14 Sept 2018

Hong-Ou-Mandel Manifolds: Robust Two-Photon “Bunching”

$$\text{HOMM: } tt' + ss' = \mathbf{0} \rightarrow |\kappa|^2 + |\gamma|^2 + |\kappa|^2|\gamma|^2 + 2\text{Re}(\eta\tau e^{i\theta}) = 2$$

A Two-Dimensional HOMM: Constraint: $P(1,1) = 0$



This figure was featured in the Physical Review A online Kaleidoscope
c. April 2014

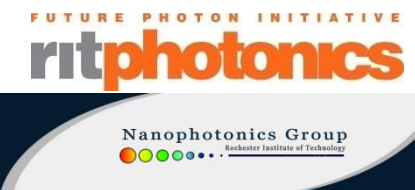
Outline

- The Goal
- Input/Output Theory: A General Solution Under Ideal Conditions
- Hong-Ou-Mandel Manifolds: A Promising Result
- **Formulation of a Quantum Optical Circuit Theory**
- A Scalable KLM CNOT Gate!?
- Engineering and Design: The Fine Print
- Summary and Outlook



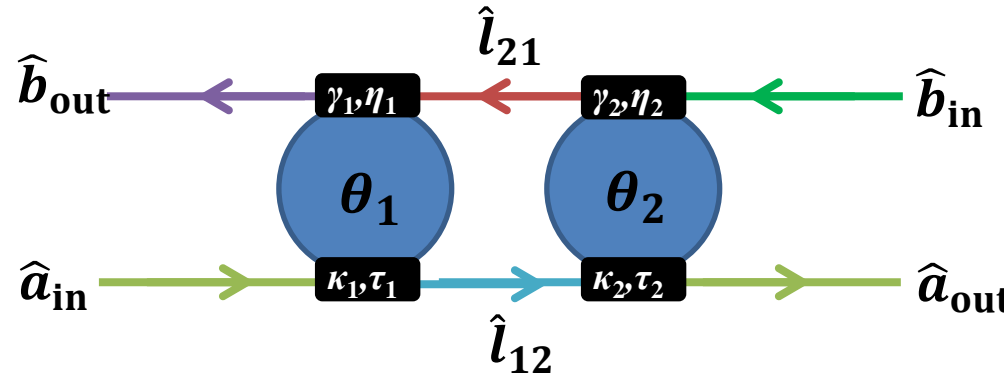
23 Jan 2019

PfQ



30

The Ring Resonator “Circuit Theory”



Notation: $\begin{pmatrix} \hat{c}_{\text{out}} \\ \hat{d}_{\text{out}} \end{pmatrix} = \begin{pmatrix} A & B \\ C & D \end{pmatrix} \begin{pmatrix} \hat{c}_{\text{in}} \\ \hat{d}_{\text{in}} \end{pmatrix}$

“Block 1”

“Block 2”

We have: $\begin{pmatrix} \hat{b}_{\text{out}} \\ \hat{l}_{12} \end{pmatrix} = \begin{pmatrix} A & B \\ C & D \end{pmatrix} \begin{pmatrix} \hat{l}_{21} \\ \hat{a}_{\text{in}} \end{pmatrix}$ $\begin{pmatrix} \hat{l}_{21} \\ \hat{a}_{\text{out}} \end{pmatrix} = \begin{pmatrix} F & G \\ H & J \end{pmatrix} \begin{pmatrix} \hat{b}_{\text{in}} \\ \hat{l}_{12} \end{pmatrix}$

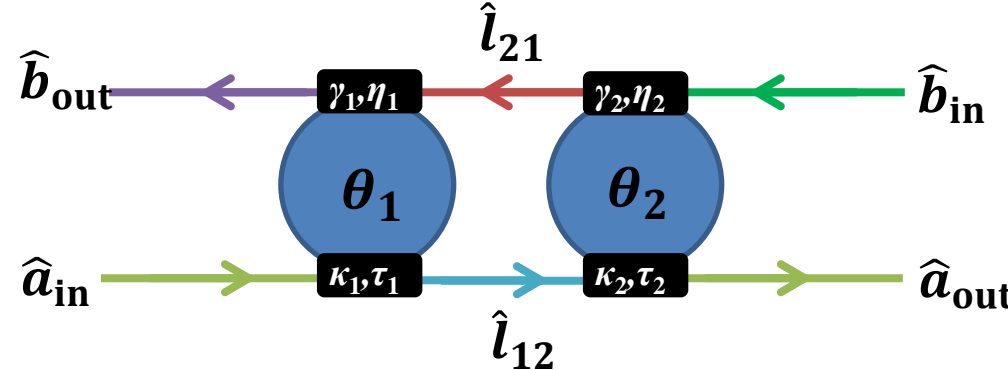
Overall Network

We want: $\begin{pmatrix} \hat{b}_{\text{out}} \\ \hat{a}_{\text{out}} \end{pmatrix} = \begin{pmatrix} \mathcal{T}_{11} & \mathcal{T}_{12} \\ \mathcal{T}_{21} & \mathcal{T}_{22} \end{pmatrix} \begin{pmatrix} \hat{b}_{\text{in}} \\ \hat{a}_{\text{in}} \end{pmatrix}$

We Introduce a set of “Mode Swap” Transformations ...



“Mode Swap” Transformation



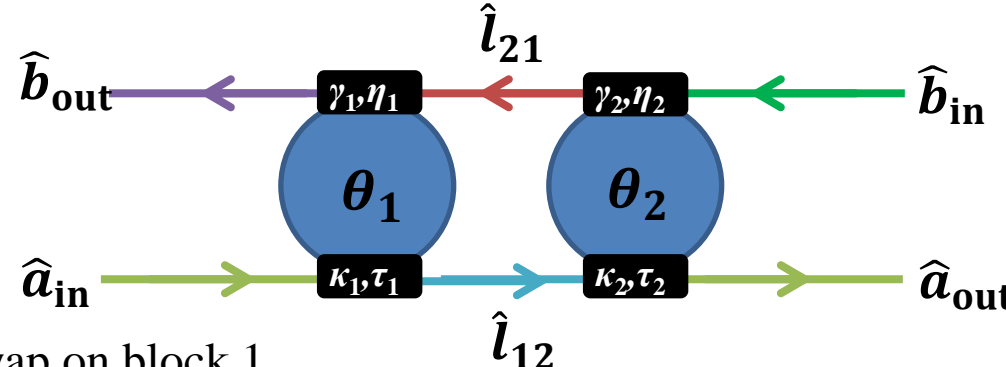
Upper “Rail” $\begin{pmatrix} \hat{c}_{\text{out}} \\ \hat{d}_{\text{out}} \end{pmatrix} = \begin{pmatrix} A & B \\ C & D \end{pmatrix} \begin{pmatrix} \hat{c}_{\text{in}} \\ \hat{d}_{\text{in}} \end{pmatrix} \rightarrow \begin{pmatrix} \hat{c}_{\text{in}} \\ \hat{d}_{\text{out}} \end{pmatrix} = \begin{pmatrix} A' & B' \\ C' & D' \end{pmatrix} \begin{pmatrix} \hat{c}_{\text{out}} \\ \hat{d}_{\text{in}} \end{pmatrix}$

Lower “Rail” $\begin{pmatrix} \hat{c}_{\text{out}} \\ \hat{d}_{\text{out}} \end{pmatrix} = \begin{pmatrix} A & B \\ C & D \end{pmatrix} \begin{pmatrix} \hat{c}_{\text{in}} \\ \hat{d}_{\text{in}} \end{pmatrix} \rightarrow \begin{pmatrix} \hat{c}_{\text{out}} \\ \hat{d}_{\text{in}} \end{pmatrix} = \begin{pmatrix} A'' & B'' \\ C'' & D'' \end{pmatrix} \begin{pmatrix} \hat{c}_{\text{in}} \\ \hat{d}_{\text{out}} \end{pmatrix}$

$$A' = \frac{1}{A}, B' = -\frac{B}{A}, C' = \frac{C}{A}, D' = \frac{1}{A} \det \begin{pmatrix} A & B \\ C & D \end{pmatrix} \quad \text{Upper Rail}$$

$$A'' = \frac{1}{D} \det \begin{pmatrix} A & B \\ C & D \end{pmatrix}, B'' = \frac{B}{D}, C'' = -\frac{C}{D}, D'' = \frac{1}{D} \quad \text{Lower Rail}$$

Quantum Transfer Function for Circuit



- local upper swap on block 1

$$\begin{pmatrix} \hat{b}_{\text{out}} \\ \hat{l}_{12} \end{pmatrix} = \begin{pmatrix} A & B \\ C & D \end{pmatrix} \begin{pmatrix} \hat{l}_{21} \\ \hat{a}_{\text{in}} \end{pmatrix} \rightarrow \begin{pmatrix} \hat{l}_{21} \\ \hat{l}_{12} \end{pmatrix} = \begin{pmatrix} A' & B' \\ C' & D' \end{pmatrix} \begin{pmatrix} \hat{b}_{\text{out}} \\ \hat{a}_{\text{in}} \end{pmatrix}$$

- local upper swap on block 2

$$\begin{pmatrix} \hat{l}_{21} \\ \hat{a}_{\text{out}} \end{pmatrix} = \begin{pmatrix} F & G \\ H & J \end{pmatrix} \begin{pmatrix} \hat{b}_{\text{in}} \\ \hat{l}_{12} \end{pmatrix} \rightarrow \begin{pmatrix} \hat{b}_{\text{in}} \\ \hat{a}_{\text{out}} \end{pmatrix} = \begin{pmatrix} F' & G' \\ H' & J' \end{pmatrix} \begin{pmatrix} \hat{l}_{21} \\ \hat{l}_{12} \end{pmatrix}$$

- result of local swaps

$$\begin{pmatrix} \hat{b}_{\text{in}} \\ \hat{a}_{\text{out}} \end{pmatrix} = \begin{pmatrix} F' & G' \\ H' & J' \end{pmatrix} \begin{pmatrix} A' & B' \\ C' & D' \end{pmatrix} \begin{pmatrix} \hat{b}_{\text{out}} \\ \hat{a}_{\text{in}} \end{pmatrix} = \begin{pmatrix} \mathcal{S}_{11} & \mathcal{S}_{12} \\ \mathcal{S}_{21} & \mathcal{S}_{22} \end{pmatrix} \begin{pmatrix} \hat{b}_{\text{out}} \\ \hat{a}_{\text{in}} \end{pmatrix}$$

- global upper swap

$$\begin{pmatrix} \hat{b}_{\text{out}} \\ \hat{a}_{\text{out}} \end{pmatrix} = \begin{pmatrix} \mathcal{T}_{11} & \mathcal{T}_{12} \\ \mathcal{T}_{21} & \mathcal{T}_{22} \end{pmatrix} \begin{pmatrix} \hat{b}_{\text{in}} \\ \hat{a}_{\text{in}} \end{pmatrix} \quad \text{q.e.d}$$

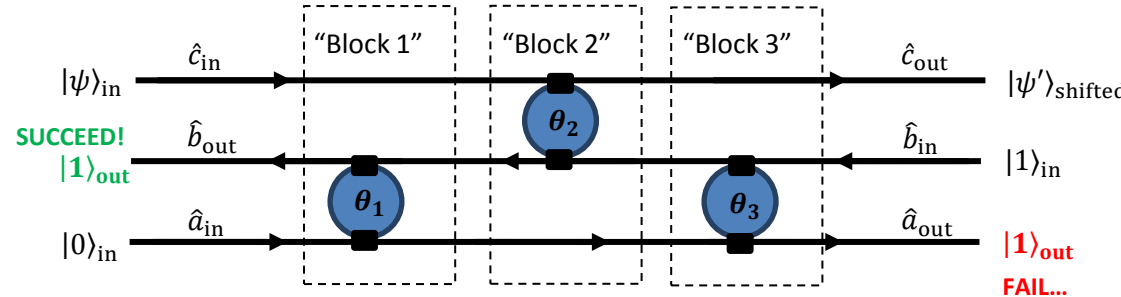
$$\mathcal{T}_{11} = \mathcal{S}'_{11}, \mathcal{T}_{12} = \mathcal{S}'_{12}, \mathcal{T}_{21} = \mathcal{S}'_{21}, \mathcal{T}_{22} = \mathcal{S}'_{22}$$



14 Sept 2018

A Ring Resonator Based Nonlinear Phase Shifter

Many adjustable, controllable parameters to search ...



Local Swaps

$$\begin{pmatrix} \hat{c}_{in} \\ \hat{b}_{out} \\ \hat{l}_{13} \end{pmatrix} = \begin{pmatrix} 1 & 0 & 0 \\ 0 & A & B \\ 0 & C & D \end{pmatrix} \begin{pmatrix} \hat{c}_{in} \\ \hat{l}_{21} \\ \hat{a}_{in} \end{pmatrix} \rightarrow \begin{pmatrix} \hat{c}_{in} \\ \hat{l}_{21} \\ \hat{l}_{13} \end{pmatrix} = \begin{pmatrix} 1 & 0 & 0 \\ 0 & A' & B' \\ 0 & C' & D' \end{pmatrix} \begin{pmatrix} \hat{c}_{in} \\ \hat{b}_{out} \\ \hat{a}_{in} \end{pmatrix}$$

$$\begin{pmatrix} \hat{c}_{out} \\ \hat{l}_{21} \\ \hat{l}_{13} \end{pmatrix} = \begin{pmatrix} P & Q & 0 \\ R & S & 0 \\ 0 & 0 & 1 \end{pmatrix} \begin{pmatrix} \hat{c}_{in} \\ \hat{l}_{32} \\ \hat{l}_{13} \end{pmatrix} \rightarrow \begin{pmatrix} \hat{c}_{out} \\ \hat{l}_{32} \\ \hat{l}_{13} \end{pmatrix} = \begin{pmatrix} P'' & Q'' & 0 \\ R'' & S'' & 0 \\ 0 & 0 & 1 \end{pmatrix} \begin{pmatrix} \hat{c}_{in} \\ \hat{l}_{21} \\ \hat{l}_{13} \end{pmatrix}$$

$$\begin{pmatrix} \hat{c}_{out} \\ \hat{l}_{32} \\ \hat{a}_{out} \end{pmatrix} = \begin{pmatrix} 1 & 0 & 0 \\ 0 & F & G \\ 0 & H & J \end{pmatrix} \begin{pmatrix} \hat{b}_{in} \\ \hat{l}_{13} \end{pmatrix} \rightarrow \begin{pmatrix} \hat{c}_{out} \\ \hat{b}_{in} \\ \hat{a}_{out} \end{pmatrix} = \begin{pmatrix} 1 & 0 & 0 \\ 0 & F' & G' \\ 0 & H' & J' \end{pmatrix} \begin{pmatrix} \hat{b}_{in} \\ \hat{l}_{32} \\ \hat{l}_{13} \end{pmatrix}$$

$$\begin{pmatrix} \hat{c}_{out} \\ \hat{b}_{in} \\ \hat{a}_{out} \end{pmatrix} = \begin{pmatrix} 1 & 0 & 0 \\ 0 & F' & G' \\ 0 & H' & J' \end{pmatrix} \begin{pmatrix} P'' & Q'' & 0 \\ R'' & S'' & 0 \\ 0 & 0 & 1 \end{pmatrix} \begin{pmatrix} 1 & 0 & 0 \\ 0 & A' & B' \\ 0 & C' & D' \end{pmatrix} \begin{pmatrix} \hat{c}_{in} \\ \hat{b}_{out} \\ \hat{a}_{in} \end{pmatrix}$$

$$= \begin{pmatrix} \alpha_{11} & \alpha_{12} & \alpha_{13} \\ \alpha_{21} & \alpha_{22} & \alpha_{23} \\ \alpha_{31} & \alpha_{32} & \alpha_{33} \end{pmatrix} \begin{pmatrix} \hat{c}_{in} \\ \hat{b}_{out} \\ \hat{a}_{in} \end{pmatrix}$$

Global Middle Rail Swap

$$\begin{pmatrix} \hat{c}_{out} \\ \hat{b}_{in} \\ \hat{a}_{out} \end{pmatrix} = \begin{pmatrix} \alpha_{11} & \alpha_{12} & \alpha_{13} \\ \alpha_{21} & \alpha_{22} & \alpha_{23} \\ \alpha_{31} & \alpha_{32} & \alpha_{33} \end{pmatrix} \begin{pmatrix} \hat{c}_{in} \\ \hat{b}_{out} \\ \hat{a}_{in} \end{pmatrix} \rightarrow \begin{pmatrix} \hat{c}_{out} \\ \hat{b}_{out} \\ \hat{a}_{out} \end{pmatrix} = \frac{1}{\alpha_{22}} \begin{pmatrix} M_{33} & \alpha_{12} & -M_{31} \\ -\alpha_{21} & 1 & -\alpha_{23} \\ -M_{13} & \alpha_{32} & M_{11} \end{pmatrix} \begin{pmatrix} \hat{c}_{in} \\ \hat{b}_{in} \\ \hat{a}_{in} \end{pmatrix}$$

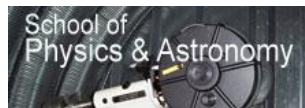


23 Jan 2019

PfQ

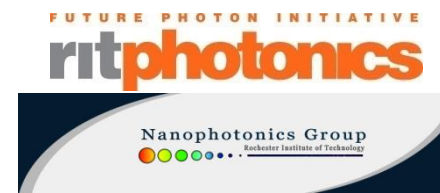
Outline

- The Goal
- Essential Ideas About Quantum Optics/Information
- Input/Output Theory: A General Solution Under Ideal Conditions
- Hong-Ou-Mandel Manifolds: A Promising Result
- Formulation of a Quantum Optical Circuit Theory
- **A Scalable KLM CNOT Gate!?**
- Engineering and Design: The Fine Print
- Summary and Outlook



23 Jan 2019

PfQ



35

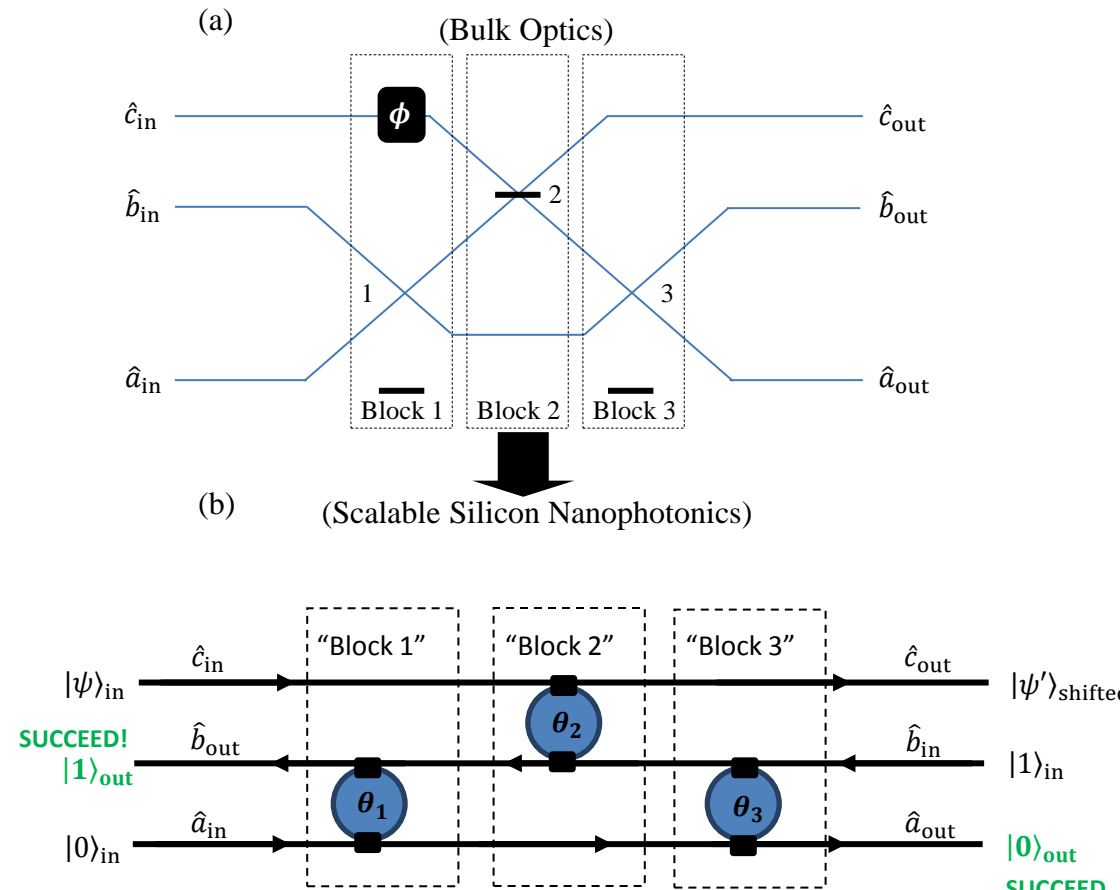
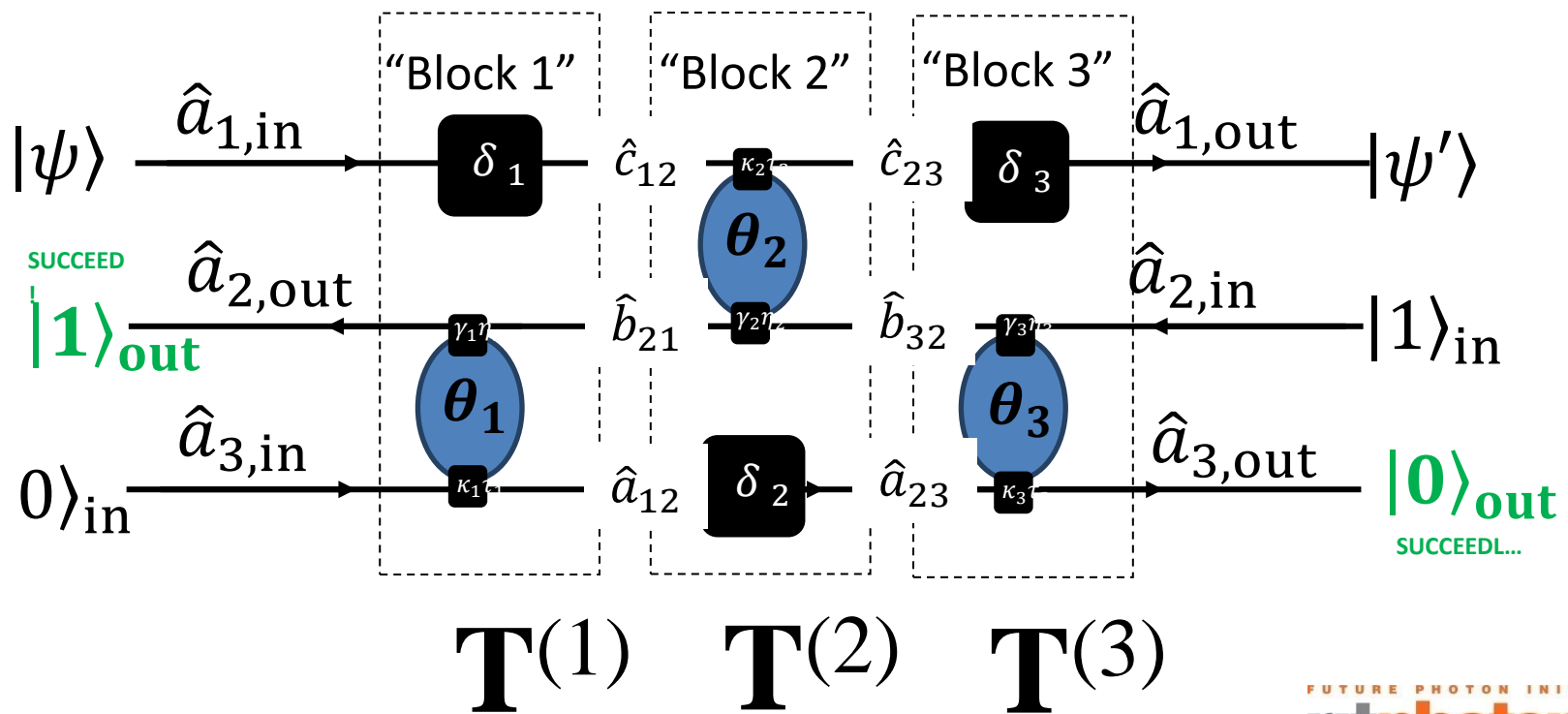


Figure 2 A schematic diagram of a NonLinear Sign Gate (a) in bulk optics and (b) as implemented via our proposal using directionally coupled silicon nanophotonics waveguides and microring resonators (mrr). The nonlinear sign flip is effected on the state in mode c , as given in Eq. (1); modes a and b are auxiliary modes required for the probabilistic action of the gate. The black arrow connecting parts (a) and (b) of the figure effectively summarizes the advancement we discuss in detail in this paper.

Our Proposal for the Essential Piece of a Scalable KLM CNOT Gate ...

A Ring Resonator Based NonLinear Phase Shifter (NLPS)



23 Jan 2019

The NonLinear Phase Shifter (we'll have two, please)

What it does: $|\psi\rangle = \alpha_0|0\rangle + \alpha_1|1\rangle + \alpha_2|2\rangle \xrightarrow{\text{NLPS}} |\psi'\rangle = \alpha_0|0\rangle + \alpha_1|1\rangle - \alpha_2|2\rangle$

How it works (when it works):

$$|\Psi\rangle = |\psi\rangle_1 \otimes |1\rangle_2 \otimes |0\rangle_3 \xrightarrow{\text{Unitary}} |\Psi'\rangle = \hat{U}|\Psi\rangle = \beta|\Psi^{\text{NLPS}}\rangle + \sqrt{1-|\beta|^2}|\Psi^\perp\rangle \xrightarrow{\text{Projection}} |\Psi^{\text{NLPS}}\rangle = \frac{\hat{P}^{\text{NLPS}}|\Psi'\rangle}{\sqrt{\langle\Psi'|\hat{P}^{\text{NLPS}}|\Psi'\rangle}}$$

How often it works: $p_{\text{success}}^{\text{NLPS}} = \langle\Psi'|\hat{P}^{\text{NLPS}}|\Psi'\rangle = |\beta|^2$

Unitary Part:

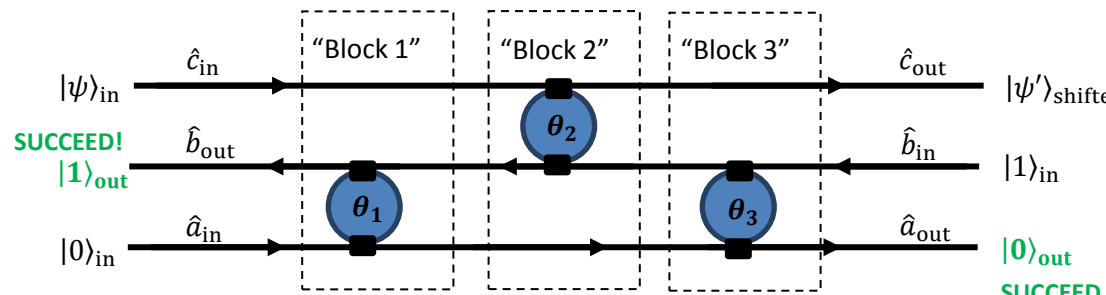
$$\begin{pmatrix} \hat{a}_{1,\text{in}}^\dagger \\ \hat{a}_{2,\text{in}}^\dagger \\ \hat{a}_{3,\text{in}}^\dagger \end{pmatrix} = \mathbf{S}^T \begin{pmatrix} \hat{a}_{1,\text{out}}^\dagger \\ \hat{a}_{2,\text{out}}^\dagger \\ \hat{a}_{3,\text{out}}^\dagger \end{pmatrix}$$

“DPI” Formulation:

$$\begin{pmatrix} \hat{a}_{1,\text{out}} \\ \hat{a}_{2,\text{out}} \\ \hat{a}_{3,\text{out}} \end{pmatrix} = \tilde{\mathcal{S}}_2^{(3)} \left[\tilde{\mathcal{S}}_2^{(3)} \left[\mathbf{T}^{(3)} \right] \tilde{\mathcal{S}}_2^{(3)} \left[\mathbf{T}^{(2)} \right] \tilde{\mathcal{S}}_2^{(3)} \left[\mathbf{T}^{(1)} \right] \right] \begin{pmatrix} \hat{a}_{1,\text{in}} \\ \hat{a}_{2,\text{in}} \\ \hat{a}_{3,\text{in}} \end{pmatrix}$$

Mode Swap Algebra:

$$\tilde{\mathcal{S}}_1^{(3)}[G] \equiv \frac{1}{g_{11}} \begin{pmatrix} 1 & -g_{12} & -g_{13} \\ g_{21} & m_{3,3} & m_{3,2} \\ g_{31} & m_{2,3} & m_{2,2} \end{pmatrix} \quad \tilde{\mathcal{S}}_2^{(3)}[G] \equiv \frac{1}{g_{22}} \begin{pmatrix} m_{3,3} & g_{12} & -m_{3,1} \\ -g_{21} & 1 & -g_{23} \\ -m_{1,3} & g_{32} & m_{1,1} \end{pmatrix} \quad \tilde{\mathcal{S}}_3^{(3)}[G] \equiv \frac{1}{g_{33}} \begin{pmatrix} m_{2,2} & m_{2,1} & g_{13} \\ m_{1,2} & m_{1,1} & g_{23} \\ -g_{31} & -g_{32} & 1 \end{pmatrix}$$



FUTURE PHOTON INITIATIVE
ritphotonics

Nanophotonics Group
Rochester Institute of Technology



23 Jan 2019

Case 1: On-resonance, no phase delays:

$$\delta_i = 0, \theta_i = 2\pi, t_i = t_i^*$$

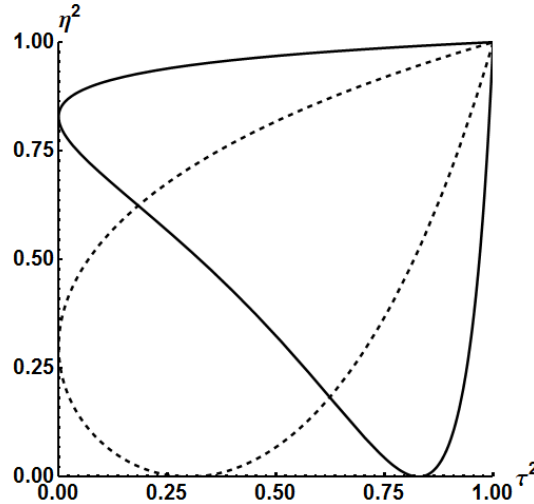
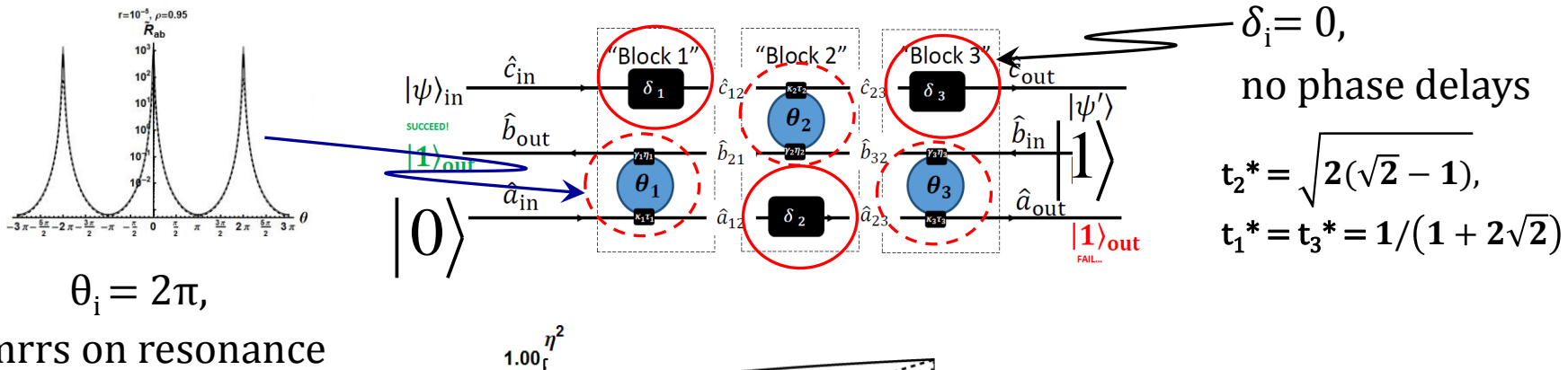
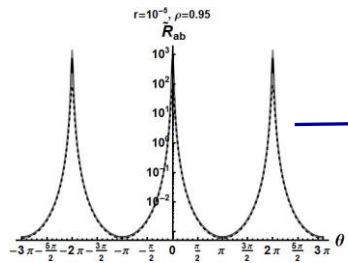


Figure 3: The one dimensional manifolds $\eta_i^2(\tau_i; T_i)$ vs τ_i^2 ($i = \{1,3\}$, black solid; $i = 2$, black dashed) from Eq. 57 on which optimal operation of the scalable NLPSG occurs under conditions of resonant ($\theta_i=0 \text{mod}2\pi$), balanced mrrs and $\delta_i=0 \text{mod}2\pi$ phase shifts in the waveguides. In contrast with bulk optical realizations, these curves provide theoretical evidence for vastly enhanced flexibility in implementation and integration of the NLPSG based on directionally coupled mrrs in silicon nanophotonics.

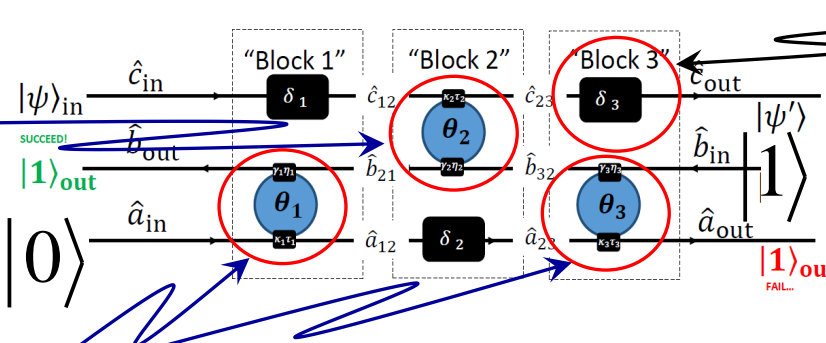
Case 2: Outer MRR *not* on resonance

$$\delta_i = 0, \quad \theta_2 = 2\pi, \quad \theta_{1,3} \neq 2\pi, \quad t_i = t_i^*$$



$\theta_2 = 2\pi$, on resonance

$\theta_{1,3} = 2\pi$, not on resonance

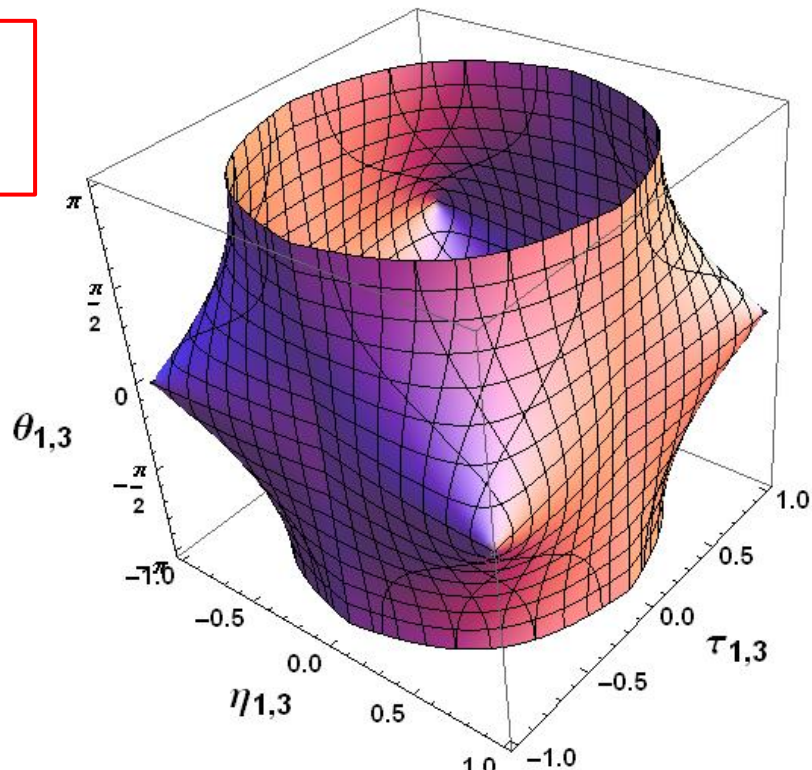


$\delta_i = 0,$
no phase delays

$$t_2^* = \sqrt{2(\sqrt{2}-1)},$$

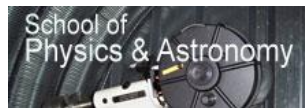
$$t_1^* = t_3^* = 1/(1+2\sqrt{2})$$

$$\text{Surface } (t_{1,3}^*)^2 \equiv \frac{\eta^2 + \tau^2 - 2 |\eta| |\tau| \cos[\theta]}{1 + \eta^2 \tau^2 - 2 |\eta| |\tau| \cos[\theta]}$$



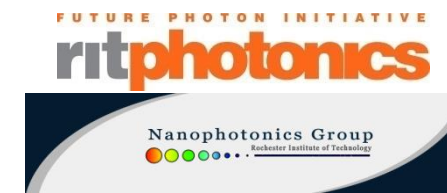
Outline

- The Goal
- Essential Ideas About Quantum Optics/Information
- Input/Output Theory: A General Solution Under Ideal Conditions
- Hong-Ou-Mandel Manifolds: A Promising Result
- Formulation of a Quantum Optical Circuit Theory
- A Scalable KLM CNOT Gate!?
- **Engineering and Design: The Fine Print**
- Summary and Outlook

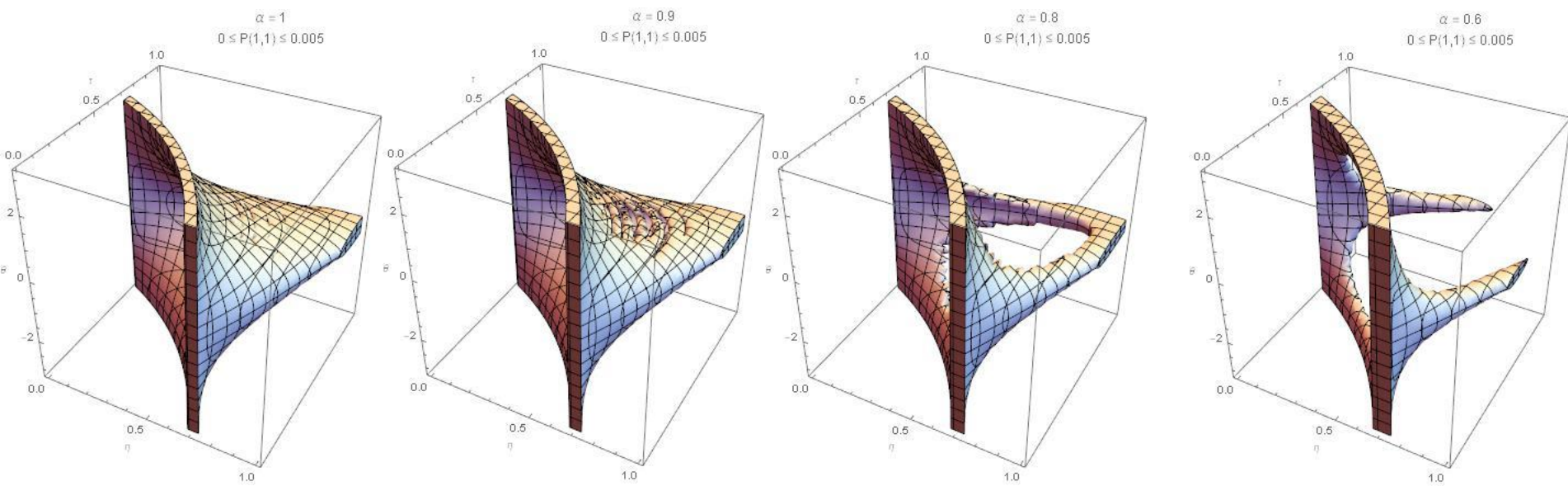


23 Jan 2019

PfQ



41

Increasing Losses (decreasing effective α) →

Theoretical analysis of losses (“whistles” and spectral effects (bells)):

P.M. Alsing, EEHIII, C. C. Tison, and A. M. Smith, *Phys. Rev. A***95**, 053828 (2017)

Theoretical analysis of photon pair generation (all the whistles and bells):

P.M. Alsing and EEHIII, *Phys. Rev. A***96**, 033847 (2017)

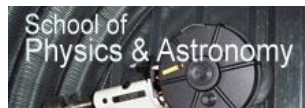
P.M. Alsing and EEHIII, *Phys. Rev. A***96**, 033848 (2017)



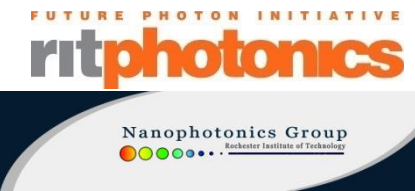
23 Jan 2019

Outline

- The Goal
- Essential Ideas About Quantum Optics/Information
- Input/Output Theory: A General Solution Under Ideal Conditions
- Hong-Ou-Mandel Manifolds: A Promising Result
- Formulation of a Quantum Optical Circuit Theory
- A Scalable KLM CNOT Gate!?
- **Engineering and Design: The Fine Print**
- **Summary and Outlook**



14 Sept 2018



43

Summary

- Ring resonators in silicon nanophotonics offer a promising architecture for quantum information processing devices (scalable, tunable, “easy” to fabricate)
- Passive Quantum Optical Feedback leads to a “topological” enhancement of the parameter space of this class of device – first example: Hong-Ou-Mandel Manifolds (HOMM)
- The existence of Hong-Ou-Mandel Manifolds (HOMM) suggest that there are robust regimes for operating quantum information processors based on ring resonator technology
- We now have a systematic way to formulate and search the parameter spaces of these systems under realistic conditions with respect to finite pulse widths and environmental losses

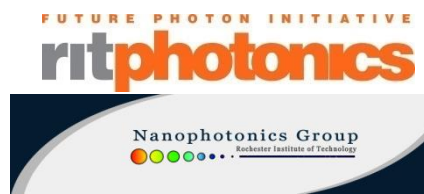
Outlook

- There are many quantum gates and networks that could be pivotal to quantum information processing, communications, metrology, and imaging – we are starting with the KLM CNOT
- We are working to develop numerical device design software to inform the planning and assembly of experimental tests of our theoretical results, and, from there, to better inform device design and integration
- **Do you have any ideas for interesting quantum optical systems to investigate? We love to collaborate!**



23 Jan 2019

PfQ



Nanophotonics Group
Rochester Institute of Technology

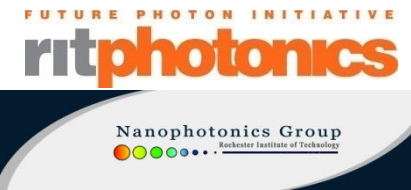
44

Thank You for Listening!



23 Jan 2019

PfQ



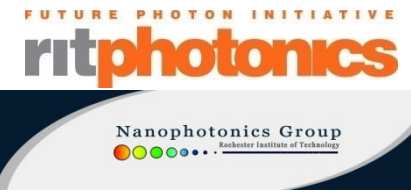
45

Back-Up Slides



23 Jan 2019

PfQ



46

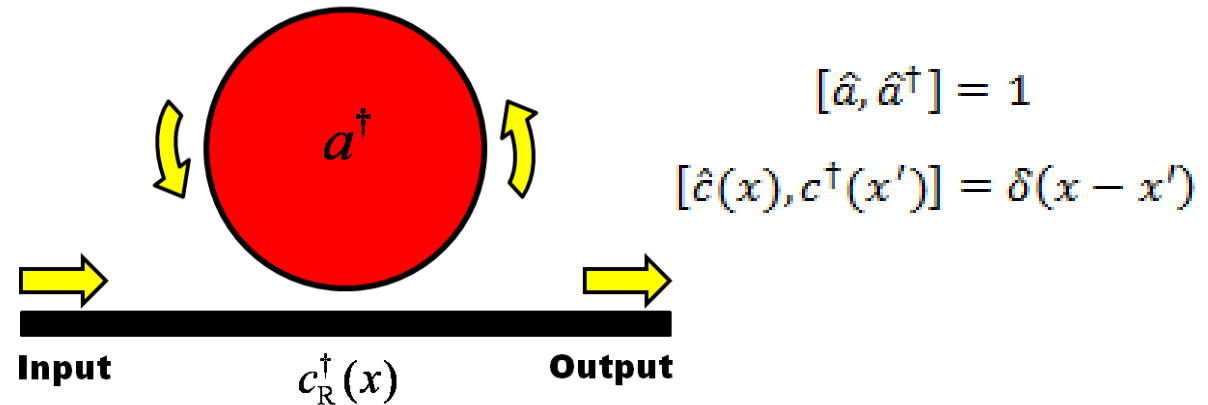


M.S. and Professional Master's Programs
Coming Fall 2019

<https://www.rit.edu/programs/physics-ms>

Single Photon Transport: Quantum Dynamics

(Scattering Theory Approach)



$$\hat{H}_{\text{eff}} = \int dx c^+(x) \left(\omega_0 - i v_g \frac{\partial}{\partial x} \right) c(x) + \left(\omega_c - i \frac{1}{\tau_c} \right) \hat{a}^\dagger \hat{a} + \int dx \delta(x) [V c^+(x) \hat{a} + V^* \hat{a}^\dagger c(x)]$$

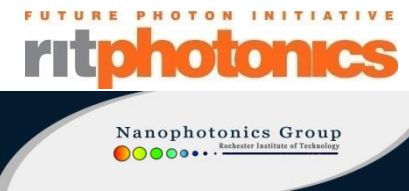
$$i \frac{\partial}{\partial t} |\Phi_1(t)\rangle = \hat{H}_{\text{eff}} |\Phi_1(t)\rangle$$

$$|\Phi_1(t)\rangle = \left(\int dx \tilde{\phi}(x, t) \hat{c}^+(x) + \tilde{e}_{\text{cav}}(t) \hat{a}^\dagger \right) |0,0\rangle$$



14 Sept 2018

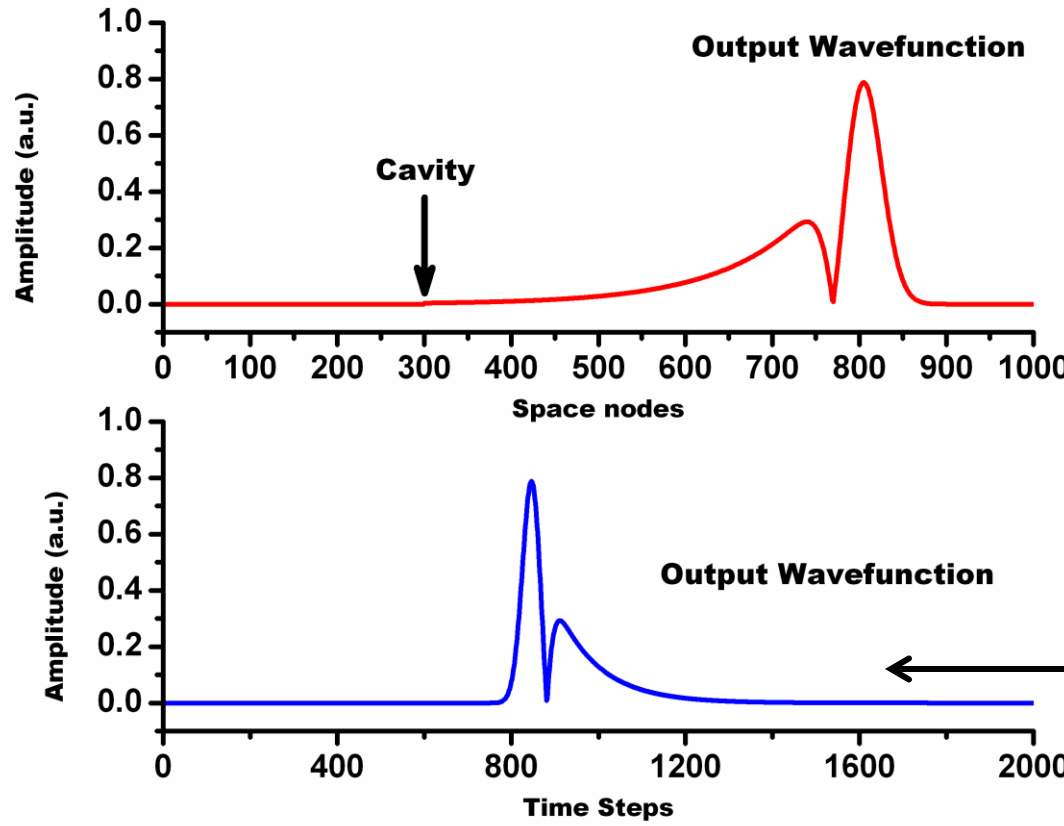
EEHIII, A.W. Elshaari, & S.F. Preble, *Phys. Rev. A* **82**, 063839(2010)



Nanophotonics Group
Rochester Institute of Technology

Single Photon Transport: Quantum Dynamics

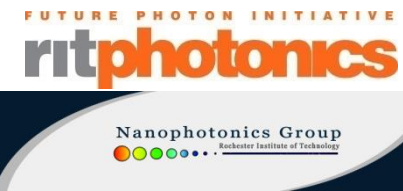
Finite Difference Time Domain Results: Wave Packet



$$\alpha|1_{\text{direct}}\rangle + \alpha|1_{\text{delay}}\rangle$$



14 Sept 2018



49

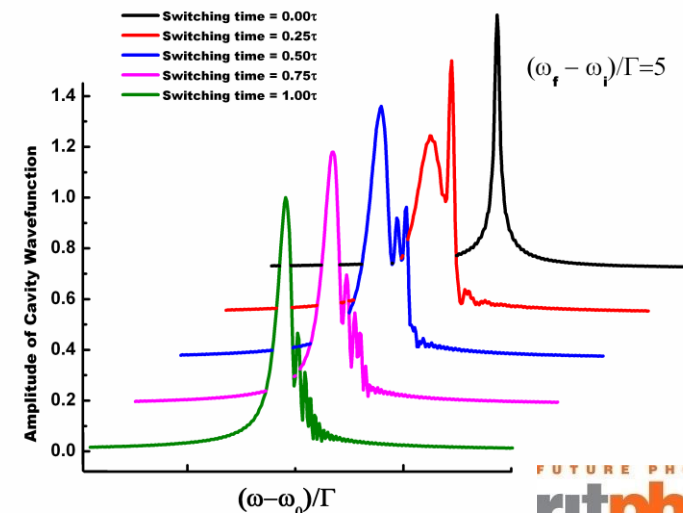
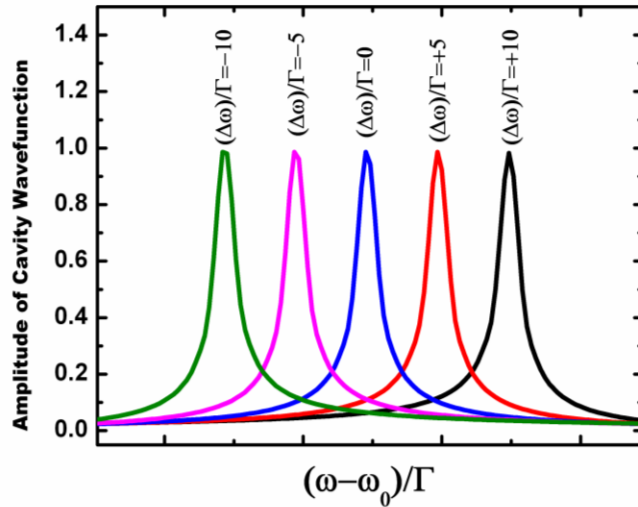
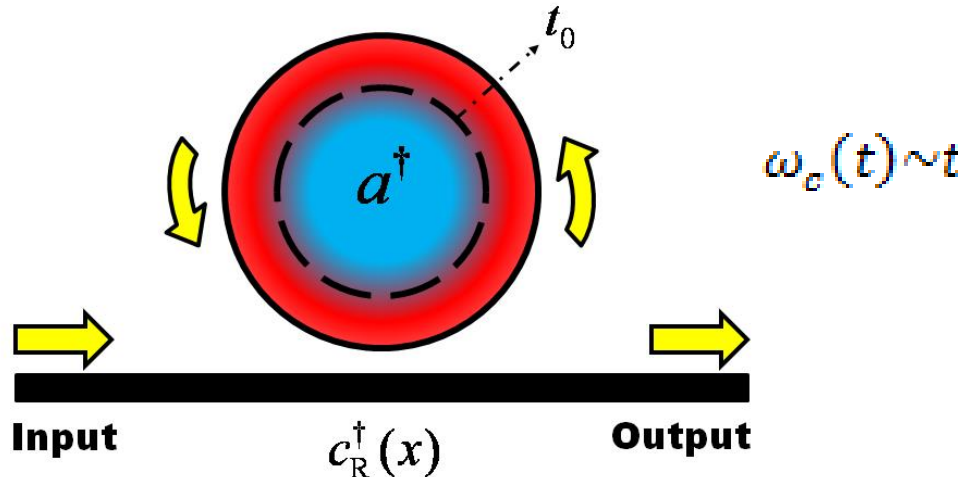
Single Photon Transport: Quantum Dynamics

Finite Difference Time Domain Results: Adiabatic Wavelength Change

Adiabatic Invariant:

$$\oint pdq = \frac{U}{\omega} = N\hbar$$

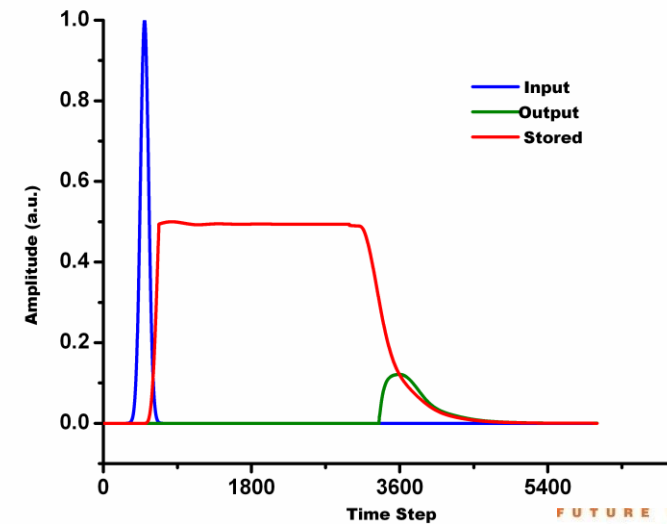
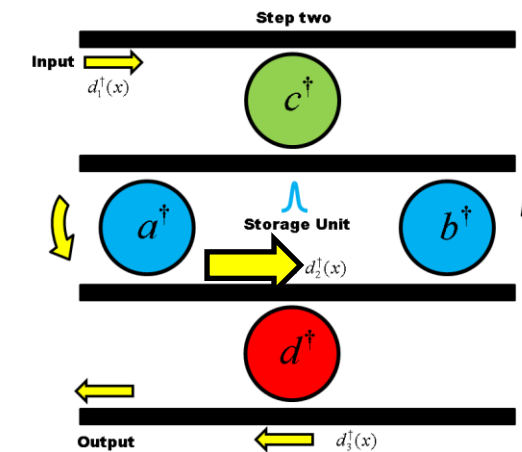
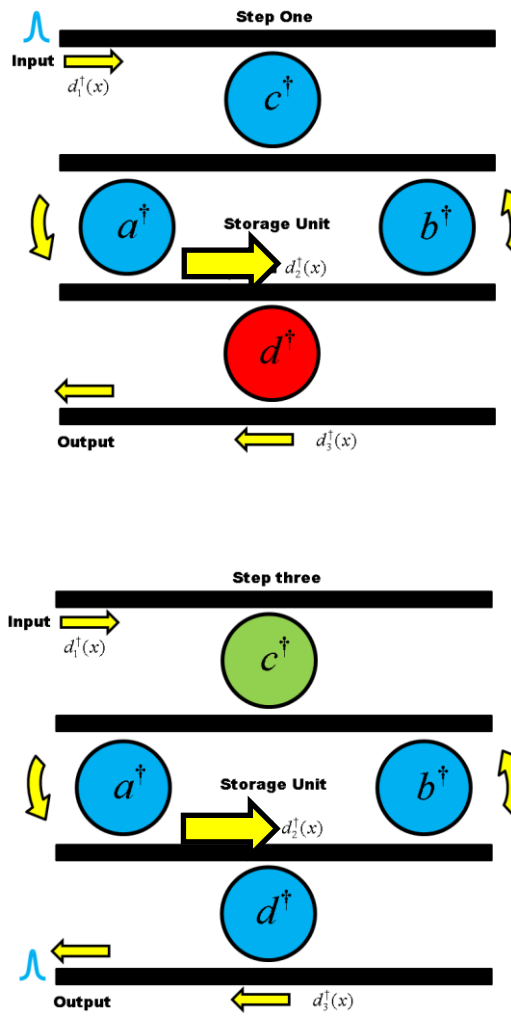
$$\therefore \frac{\Delta\lambda}{\lambda} = \frac{\Delta U}{U}$$



14 Sept 2018

Single Photon Transport: Quantum Dynamics

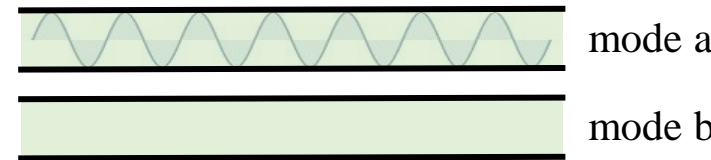
Single Photon Storage: Toward Quantum Memory



FUTURE PHOTON INITIATIVE
ritphotonics



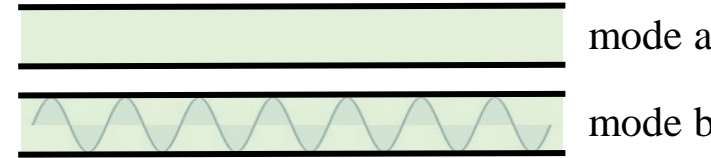
Logical {1}



mode a

mode b

Logical {0}



mode a

mode b

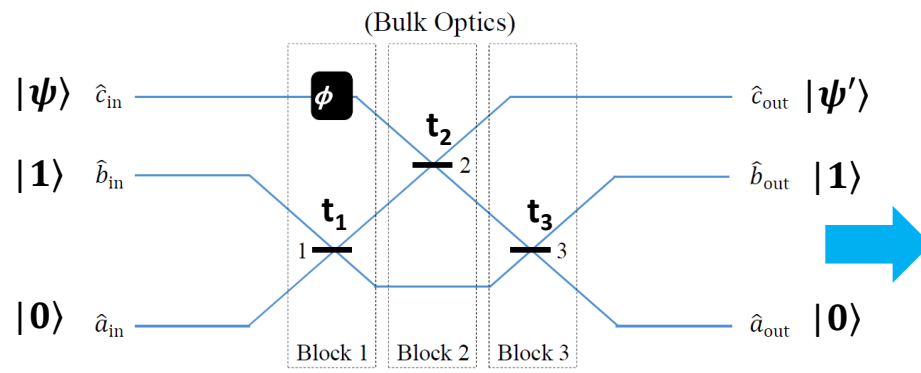
Outline

- KLM Design for Nonlinear Sign Gate with beam splitters
 - Essential element of KLM CNOT gate
- NLSG design with mrr
 - Review of single-bus and double-bus mrr,
 - Extension of dimension of parameter space by using; HOM Manifolds
 - Results
- Papers
 - Raymer, M. and McKinstry, C., "*Quantum input-output theory for optical cavities with arbitrary coupling strength: application to two-photon wave-packet shaping*," Phys. Rev. A 88, 043819 (2013)
 - E. E. Hach III, S. F. Preble, A. W. Elshaari, P. M. Alsing, and M. L. Fanto, "*Scalable Hong-Ou-Mandel manifolds in quantum-optical ring resonators*," Phys. Rev. A 89, 043805 (2014).
 - Alsing, P. M., Hach III, E. E., Tison, C. C., and Smith, A. M., "*A quantum optical description of losses in ring resonators based on field operator transformations*," Phys. Rev. A 95, 053828 (2017)
 - Alsing, P. M. and Hach III, E. E., "*Photon-pair generation in a lossy-microring resonator. I. Theory*," Phys. Rev. A 96 (3), 033847 (2017); ([1705.09227v2](https://arxiv.org/abs/1705.09227v2))
 - Alsing, P. M. and Hach III, E. E., "*Photon-pair generation in a lossy-microring resonator. II. Entanglement in the output mixed Gaussian squeezed state*," Phys. Rev. A 96 (3), 033848 ([1708.01338](https://arxiv.org/abs/1708.01338)) (2017)

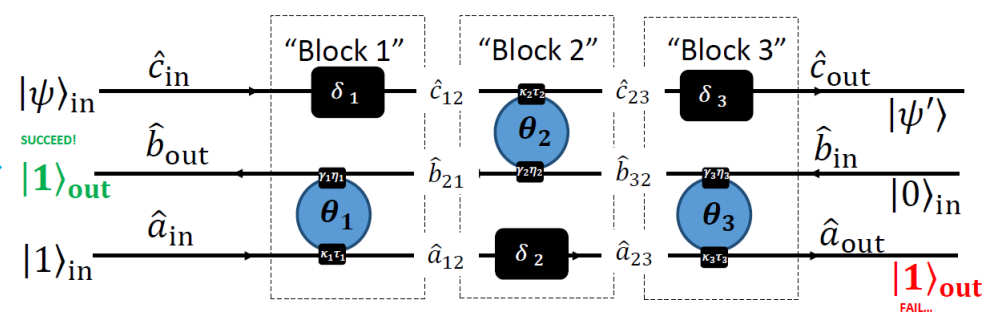
Ralph et al, PRA 95, 012314 (2017); Skaar and Ladd, Annals Phys. 321, 1185 (2004)

KLM Nonlinear Sign Gate

- Last Year (SPIE: Warsaw 2017): Nonlinear Sign Gate mrr
- Proposed KLM Nonlinear Sign Gate with mrrs
- Wider parameter range of operation (akin to HOM manifolds in mrr, in 2017 talk)



A Ring Resonator Based Nonlinear Sign Shifter

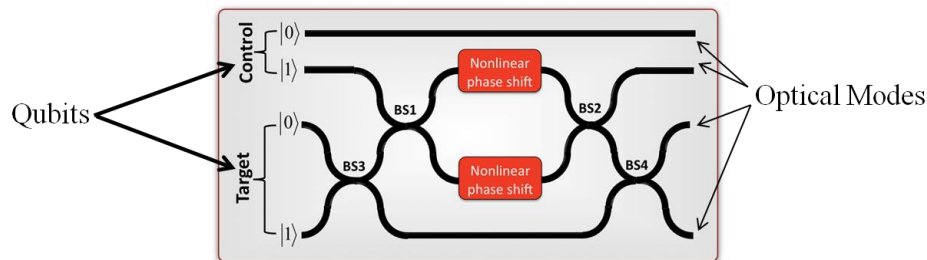


$$|\psi_{in}\rangle_c = \alpha_0 |0\rangle_c + \alpha_1 |1\rangle_c + \alpha_2 |2\rangle_c$$

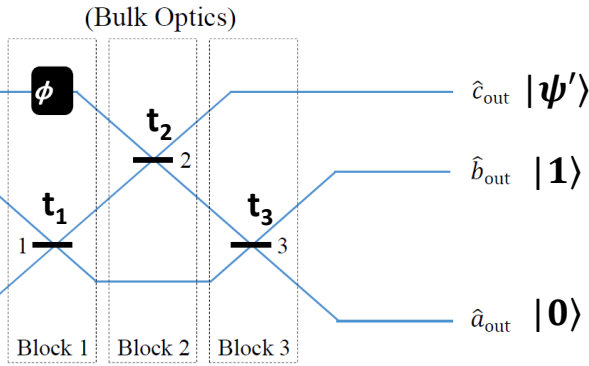
$$\xrightarrow{\text{NLS}} |\psi'_{out}\rangle_c = \alpha_0 |0\rangle_c + \alpha_1 |1\rangle_c - \alpha_2 |2\rangle_c,$$

$$t_1^* = t_3^* = \frac{1}{\sqrt{4 - 2\sqrt{2}}}, \quad t_2^* = \sqrt{2} - 1,$$

$$|\beta_{max}|^2 = 1/4$$



KLM Nonlinear Sign Gate



$$M_1 = \begin{pmatrix} t_1 e^{i\phi_1} & \sqrt{1-t_1^2} \\ \sqrt{1-t_1^2} & -t_1 e^{-i\phi_1} \end{pmatrix}, \quad M_2 = \begin{pmatrix} -t_2 e^{-i\phi_2} & \sqrt{1-t_2^2} \\ \sqrt{1-t_2^2} & t_2 e^{i\phi_2} \end{pmatrix},$$

$$M_3 = \begin{pmatrix} t_3 e^{i\phi_3} & \sqrt{1-t_3^2} \\ \sqrt{1-t_3^2} & -t_3 e^{-i\phi_3} \end{pmatrix}$$

$$\begin{aligned} \begin{pmatrix} c_{out} \\ b_{in} \\ a_{out} \end{pmatrix} &= B_3 B_2 B_1 \begin{pmatrix} c_{out} \\ b_{out} \\ a_{out} \end{pmatrix}, \\ &= \left(\begin{array}{c|cc} \frac{e^{i\delta_3}}{0} & 0 & 0 \\ \hline 0 & M_3 \end{array} \right) \left(\begin{array}{c|cc} M_2 & 0 & 0 \\ \hline 0 & \frac{0}{e^{i\delta_2}} \end{array} \right) \left(\begin{array}{c|cc} \frac{e^{i\delta_1}}{0} & 0 & 0 \\ \hline 0 & M_1 \end{array} \right) \begin{pmatrix} c_{in} \\ b_{in} \\ a_{in} \end{pmatrix}, \\ &\equiv S \begin{pmatrix} c_{in} \\ b_{in} \\ a_{in} \end{pmatrix}, \\ &= \begin{pmatrix} S_{11} & S_{12} & S_{13} \\ S_{21} & S_{22} & S_{23} \\ S_{31} & S_{32} & S_{33} \end{pmatrix} \begin{pmatrix} c_{in} \\ b_{in} \\ a_{in} \end{pmatrix}, \end{aligned}$$

$$\begin{aligned} |\Phi_{in}\rangle_{cba} &= |\psi_{in}\rangle_c |1\rangle_b |0\rangle_a, \\ &= \alpha_0 |010\rangle_{cba} + \alpha_1 |110\rangle_{cba} + \alpha_2 |210\rangle_{cba}, \\ \xrightarrow{\text{NLS}} \alpha_0 |010\rangle_{cba} + \alpha_1 |110\rangle_{cba} - \alpha_2 |210\rangle_{cba}, \\ &= |\Phi_{out}\rangle_{cba}. \end{aligned}$$

$$\text{Transition 1: } |010\rangle_{cba} \rightarrow \beta |010\rangle_{cba},$$

$$\text{Transition 2: } |110\rangle_{cba} \rightarrow \beta |110\rangle_{cba},$$

$$\text{Transition 3: } |210\rangle_{cba} \rightarrow -\beta |210\rangle_{cba},$$

$$\beta^* = S_{22} = e^{i(\phi_1+\phi_2+\phi_3)} t_1 t_2 t_3 + e^{i\delta_2} \sqrt{1-t_1^2} \sqrt{1-t_3^2},$$

$$\beta^* = \frac{1}{\sqrt{2}} S_{12} S_{21} = \frac{1}{\sqrt{2}} e^{i(\delta_1+\delta_3+\phi_1+\phi_3)} t_1 \sqrt{1-t_2^2} t_3,$$

$$S_{11} = 1 - \sqrt{2} \Rightarrow e^{i(\delta_1+\delta_3-\phi_3)} t_2 = \sqrt{2} - 1.$$

$$t_1^* = t_3^* = \frac{1}{\sqrt{4-2\sqrt{2}}}, \quad t_2^* = \sqrt{2} - 1,$$

$$|\beta_{max}|^2 = 1/4$$

Quantum Input-Output Theory for MRR

Standard Langevin Quantum I/O Theory

Wall & Milburn, *Quantum Optics* Springer (1994)

$$\dot{\hat{a}}_{int}(t) = -\frac{i}{\hbar} [\hat{a}_{int}, H_{sys}] + \frac{\gamma_c}{2} \hat{a}_{int}(t) - \sqrt{\gamma_c} \hat{a}_{out}(t)$$

$$\dot{\hat{a}}_{int}(t) = -\frac{i}{\hbar} [\hat{a}_{int}, H_{sys}] - \frac{(\gamma_c + \gamma_{int})}{2} \hat{a}_{int}(t)$$

$$+ \sqrt{\gamma_c} \hat{a}_{in}(t) + \sqrt{\gamma_{int}} \hat{f}(t)$$

Raymer & McKinstry, PRA 88, 043819 (2013)

$$(\partial_t + v_a \partial_z) a(z, t) = \alpha_{polz} P(z, t)$$

$$a(0_+, t) = \rho_a a(L_-, t) + \tau_a a_{in}(t)$$

$$a_{out}(t) = \tau_a a(L_-, t) - \rho_a a_{in}(t)$$

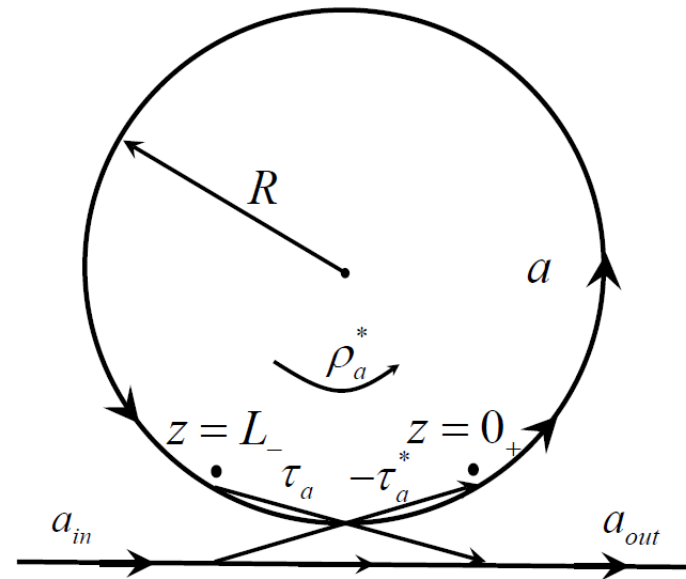
$$|\rho_a|^2 + |\tau_a|^2 = 1$$

$$a_{out}(\omega) \equiv G_{out,in}(\omega) a_{in}(\omega),$$

$$G_{out,in}(\omega) = e^{i\omega T_a} \left[\frac{1 - \rho_a e^{-i\omega T_a}}{1 - \rho_a e^{i\omega T_a}} \right]$$

$$|G_{out,in}(\omega)| = 1$$

$$a_{out}(\omega) = \left(\frac{\rho_a - \alpha_a e^{i\theta_a}}{1 - \rho_a^* \alpha_a e^{i\theta_a}} \right) a_{in}(\omega) - i|\tau_a|^2 \sqrt{\Gamma_a} \sum_{n=0}^{\infty} (\rho_a)^n \int_0^{(n+1)L} dz e^{i\xi_a(\omega)[(n+1)L-z]} \hat{s}(z, \omega)$$



Alsing, Hach, Tison, Smith, PRA 95, 053828 (2017)

$$a_{out}(\omega) = G_{out,in}(\omega) a_{in} + H_{out,in}(\omega) f_a(\omega)$$

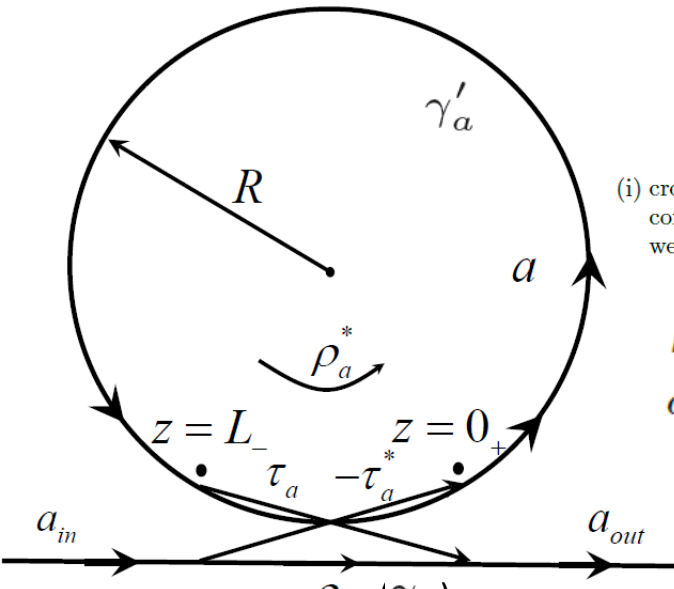
$$G_{out,in}(\omega) = \left(\frac{\rho_a - \alpha_a e^{i\theta_a}}{1 - \rho_a^* \alpha_a e^{i\theta_a}} \right)$$

$$|H_{out,in}(\omega)| = \sqrt{1 - |G_{out,in}(\omega)|^2}$$

$$a(L_-, \omega) = e^{i\xi_a(\omega)L} a(0_+, \omega) + i\sqrt{\Gamma_a(\omega)} \int_0^L dz e^{i\xi_a(\omega)(L-z)} s(z, \omega)$$

$$s(z, \omega) = \sum_{n=0}^{\infty} (\rho_a)^n \int_0^{(n+1)L} dz' e^{i\xi_a(\omega)[(n+1)L-z']} \hat{s}(z', \omega)$$

High Cavity Q Limit



Raymer & McKinstry, PRA 88, 043819 (2013)
Alsing, Hach, PRA 96, 033847 & 033848 (2017)
(see also) Schneeloch, et al., 1807.10885

(i) cross coupling τ_a is very small so that the cavity storage time is long, (ii) the cavity round trip time T_a is small compared to the duration of the input-field pulse i.e. $\omega T_a \ll 1$, and (iii) the input field is narrow band and thus well contained within a single FSR of the mrr.

$$\begin{aligned} \rho_a &\equiv e^{-\gamma_a T_a / 2} \approx 1 - \gamma_a T_a / 2, & \tau_a &= \sqrt{1 - \rho_a^2} \approx \sqrt{\gamma_a T_a}, \\ \alpha_a &= e^{-\gamma'_a T_a / 2} \approx 1 - \gamma'_a T_a / 2, & e^{i \omega T_a} &\approx 1 + i \omega T_a, \end{aligned}$$

γ_a - through coupling loss rate

γ'_a - internal propagation loss rate

T_a - cavity round trip time

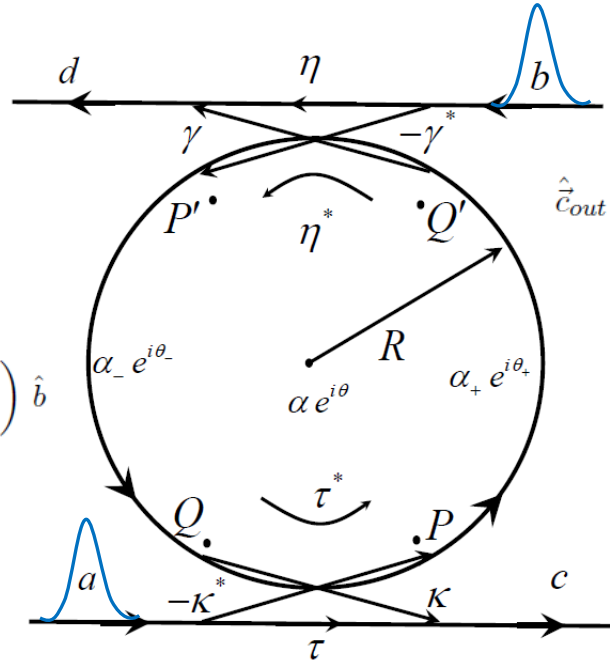
$$G_{out,in}(\omega) = \left(\frac{\rho_a - \alpha_a e^{i\theta_a}}{1 - \rho_a \alpha_a e^{i\theta_a}} \right) \xrightarrow{\text{high Q}} \frac{i\omega + (\gamma_a - \gamma'_a)/2}{-i\omega + (\gamma_a + \gamma'_a)/2},$$

$$H_{out,in}(\omega) \equiv |H_{out,in}(\omega)| = \frac{|\tau_a|^2 (1 - \alpha_a^2)}{|1 - \rho_a \alpha_a e^{i\theta_a}|^2} \xrightarrow{\text{high Q}} \frac{\sqrt{\gamma_a \gamma'_a}}{\omega^2 + [(\gamma_a + \gamma'_a)/2]^2},$$

The high cavity Q limit recovers the usual Langevin results valid near cavity resonances

Dual Rail MRR: HOM Manifolds

Alsing, Hach, PRA 96, 033847 (2017); PRA 96, 033848 (2017);



$$\hat{c} = \left(\frac{\tau - \eta^* \alpha e^{i\theta}}{1 - \tau \eta^* \alpha e^{i\theta}} \right) \hat{a} - \left(\frac{\gamma^* \kappa \sqrt{\alpha} e^{i\theta/2}}{1 - \tau \eta^* \alpha e^{i\theta}} \right) \hat{b} - i\sqrt{\Gamma} (|\kappa|^2 \eta^* \hat{f}_a + \gamma^* \kappa \hat{f}_b)$$

$$\hat{d} = - \left(\frac{\kappa^* \gamma \sqrt{\alpha} e^{i\theta/2}}{1 - \tau \eta^* \alpha e^{i\theta}} \right) \hat{a} + \left(\frac{\eta - \tau^* \alpha e^{i\theta}}{1 - \tau \eta^* \alpha e^{i\theta}} \right) \hat{b} - i\sqrt{\Gamma} (\kappa^* \gamma \hat{f}_a + |\gamma|^2 \tau^* \hat{f}_b)$$

$$\begin{aligned} \hat{\vec{c}}_{out} &= \begin{pmatrix} \hat{c} \\ \hat{d} \end{pmatrix} = \begin{pmatrix} \mathcal{A}_{a \rightarrow c} & \mathcal{A}_{b \rightarrow c} \\ \mathcal{A}_{a \rightarrow d} & \mathcal{A}_{b \rightarrow d} \end{pmatrix} \begin{pmatrix} \hat{a} \\ \hat{b} \end{pmatrix} + \begin{pmatrix} \hat{F}_c \\ \hat{F}_d \end{pmatrix} \\ &\equiv M \hat{\vec{a}}_{in} + \hat{\vec{F}}, \end{aligned}$$

HOM in MRR

$$|\Psi\rangle_{in} = |1_a, 1_b, 0_{env}\rangle = \hat{a}^\dagger \hat{b}^\dagger |0_a, 0_b, 0_{env}\rangle$$

$$\hat{\vec{a}}_{in}^\dagger = \mathcal{M} (\hat{\vec{c}}_{out}^\dagger - \hat{\vec{F}}^\dagger), \quad \mathcal{M} = M^{-1*}$$

$$|\Psi\rangle_{out} \equiv \underline{|\Psi^{(2)}\rangle_{c,d} \otimes |0\rangle_{env}} + |\phi^{(1)}\rangle_{c,d} \otimes \hat{F}_c^\dagger |0\rangle_{env} + |\varphi^{(1)}\rangle_{c,d} \otimes \hat{F}_d^\dagger |0\rangle_{env} + |0, 0\rangle_{c,d} \otimes |\Phi^{(2)}\rangle_{env}$$

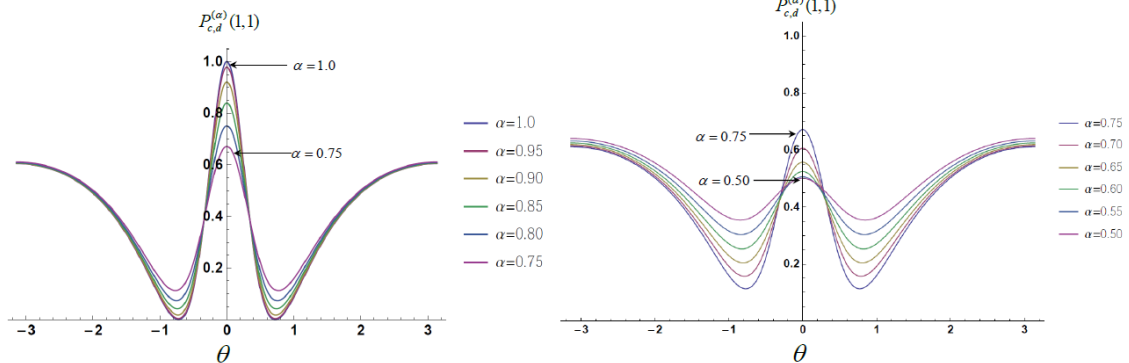
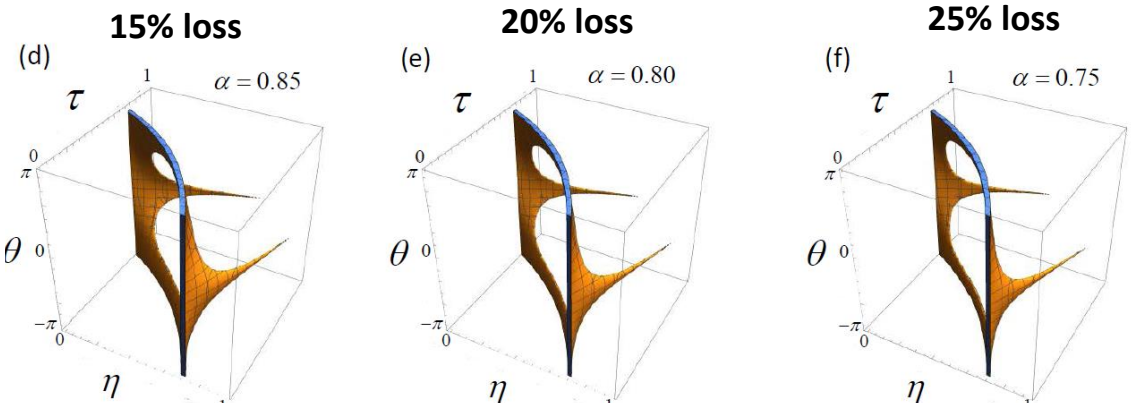
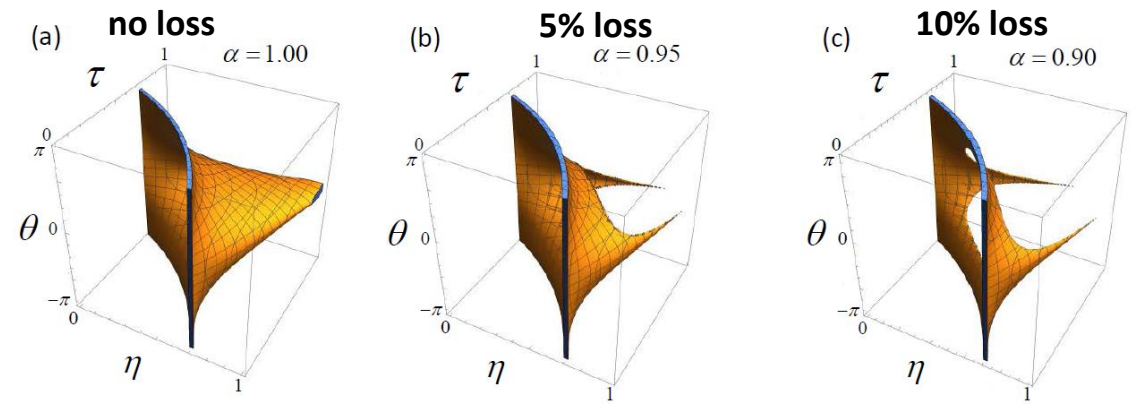
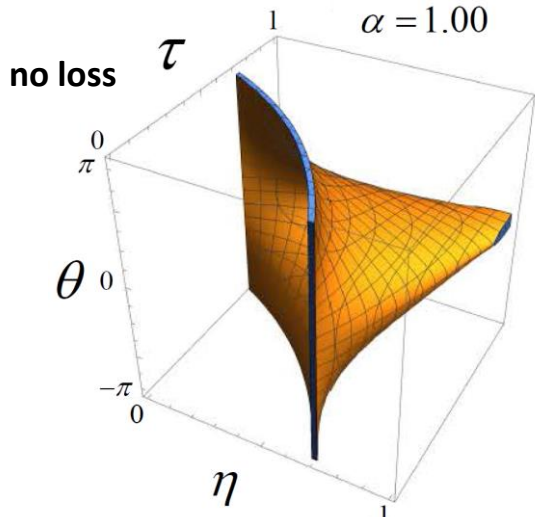
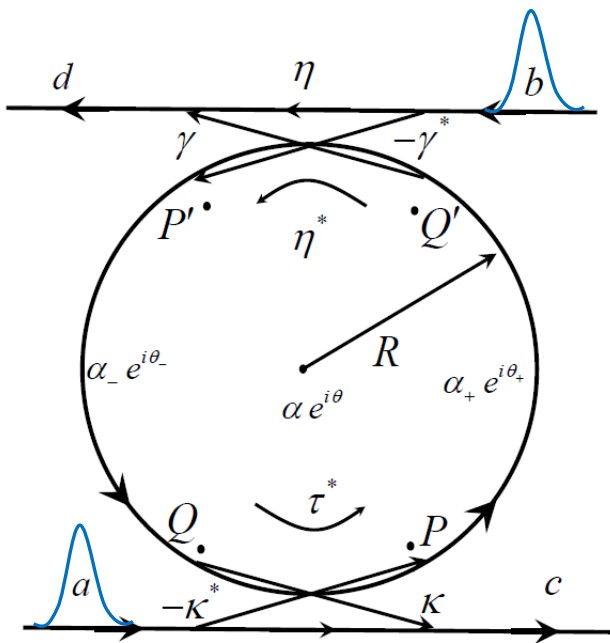
$$|\Psi^{(2)}\rangle_{c,d} = \sqrt{2} \mathcal{M}_{11} \mathcal{M}_{21} |2, 0\rangle_{c,d} + \underline{\text{Perm}(\mathcal{M}) |1, 1\rangle_{c,d}} + \sqrt{2} \mathcal{M}_{12} \mathcal{M}_{22} |0, 2\rangle_{c,d}$$

$$\text{Perm}(\mathcal{M}) \equiv \mathcal{M}_{11} \mathcal{M}_{22} + \mathcal{M}_{12} \mathcal{M}_{21}$$

Dual Bus MRR: HOM Manifolds

E. E. Hach III, *et al.*, Phys. Rev. A 89, 043805 (2014);

Alsing, P. M., *et al.* Phys. Rev. A 95, 053828 (2017)



$$\begin{aligned} |\Psi'\rangle = & \left[\alpha_0 S_{22} |0\rangle_1 + \alpha_1 (S_{11}S_{22} + S_{21}S_{12}) |1\rangle_1 + \alpha_1 S_{11} (S_{11}S_{22} + 2S_{21}S_{12}) |2\rangle_1 \right] \otimes |1\rangle_2 \otimes |0\rangle_3 \\ & + \left\{ \alpha_0 \sum_{j \neq 2} S_{j2} \hat{a}_{j,\text{out}}^\dagger + \alpha_1 \sum_{(j,k) \neq \{(1,2),(2,1)\}} S_{j1} S_{k2} \hat{a}_{j,\text{out}}^\dagger \hat{a}_{k,\text{out}}^\dagger + \frac{\alpha_2}{\sqrt{2}} \sum_{(j,k,l) \neq \{\text{perm}(1,1,2)\}} S_{j1} S_{k1} S_{l2} \hat{a}_{j,\text{out}}^\dagger \hat{a}_{k,\text{out}}^\dagger \hat{a}_{l,\text{out}}^\dagger \right\} |0,0,0\rangle \end{aligned}$$

$$\alpha_0 S_{22} = \beta \alpha_0$$

$$\alpha_1 (S_{11}S_{22} + S_{21}S_{12}) = \beta \alpha_1$$

$$\alpha_2 S_{11} (S_{11}S_{22} + 2S_{21}S_{12}) = -\beta \alpha_2$$

$$S_{11}=1-\sqrt{2}$$

$$p_{\text{success}}^{\text{NLPS}} = |\beta|^2 = |S_{22}|^2 = \tfrac{1}{2} |S_{21}|^2 |S_{12}|^2$$

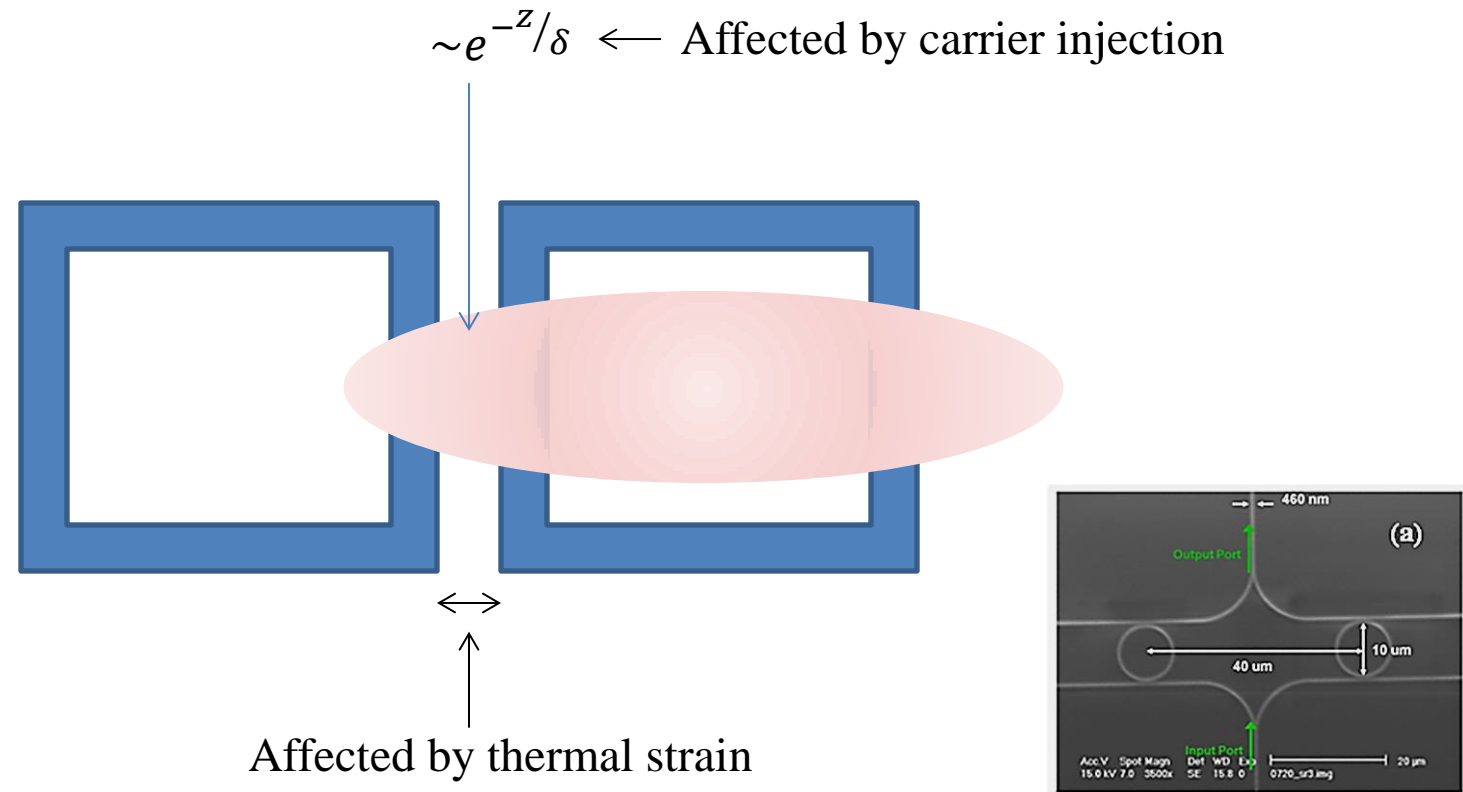


14 Sept 2018



60

Conceptual Picture of Evanescent Coupling



$$\begin{aligned} |\Psi'\rangle = & \left[\alpha_0 S_{22} |0\rangle_1 + \alpha_1 (S_{11}S_{22} + S_{21}S_{12}) |1\rangle_1 + \alpha_1 S_{11} (S_{11}S_{22} + 2S_{21}S_{12}) |2\rangle_1 \right] \otimes |1\rangle_2 \otimes |0\rangle_3 \\ & + \left\{ \alpha_0 \sum_{j \neq 2} S_{j2} \hat{a}_{j,\text{out}}^\dagger + \alpha_1 \sum_{(j,k) \neq \{(1,2),(2,1)\}} S_{j1} S_{k2} \hat{a}_{j,\text{out}}^\dagger \hat{a}_{k,\text{out}}^\dagger + \frac{\alpha_2}{\sqrt{2}} \sum_{(j,k,l) \neq \{\text{perm}(1,1,2)\}} S_{j1} S_{k1} S_{l2} \hat{a}_{j,\text{out}}^\dagger \hat{a}_{k,\text{out}}^\dagger \hat{a}_{l,\text{out}}^\dagger \right\} |0,0,0\rangle \end{aligned}$$

$$\alpha_0 S_{22} = \beta \alpha_0$$

$$\alpha_1 (S_{11}S_{22} + S_{21}S_{12}) = \beta \alpha_1$$

$$\alpha_2 S_{11} (S_{11}S_{22} + 2S_{21}S_{12}) = -\beta \alpha_2$$

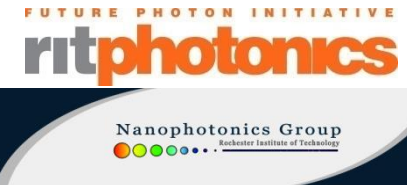
$$S_{11}=1-\sqrt{2}$$

$$p_{\text{success}}^{\text{NLPS}} = |\beta|^2 = |S_{22}|^2 = \tfrac{1}{2} |S_{21}|^2 |S_{12}|^2$$



23 Jan 2019

PfQ

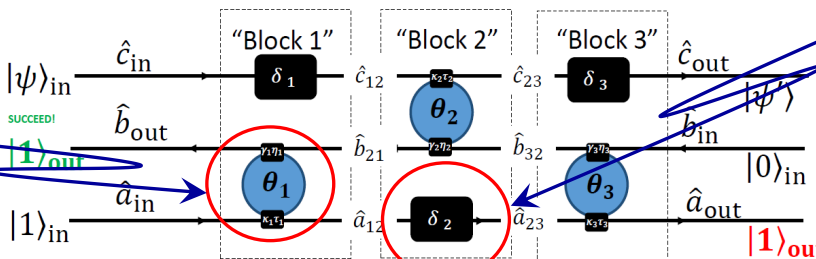
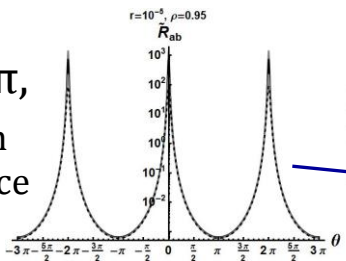


62

Case 3: vary middle interblock phase delay:

$$\delta_1 = \delta_3, \quad \delta_2 \neq 0, \quad \theta_i = 2\pi, \quad t_i = t_i^*$$

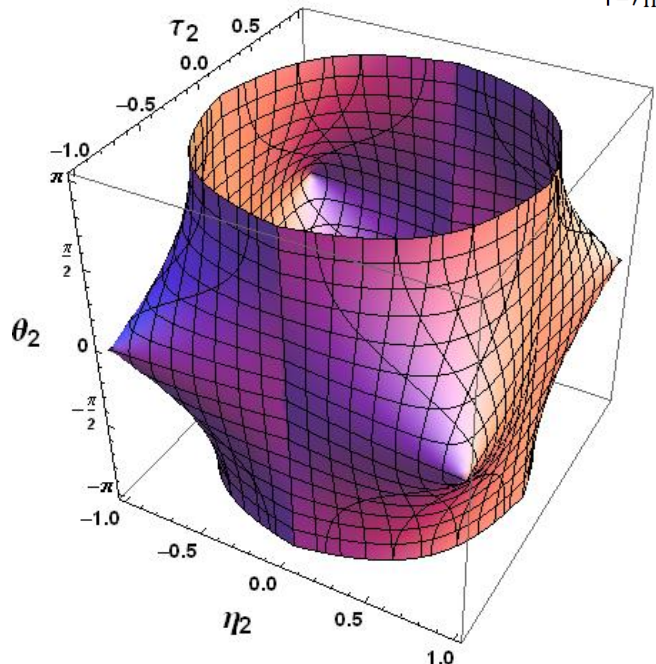
$\theta_i = 2\pi$,
mrrs on
resonance



$\delta_2 \neq 0$,
vary middle
phase delay

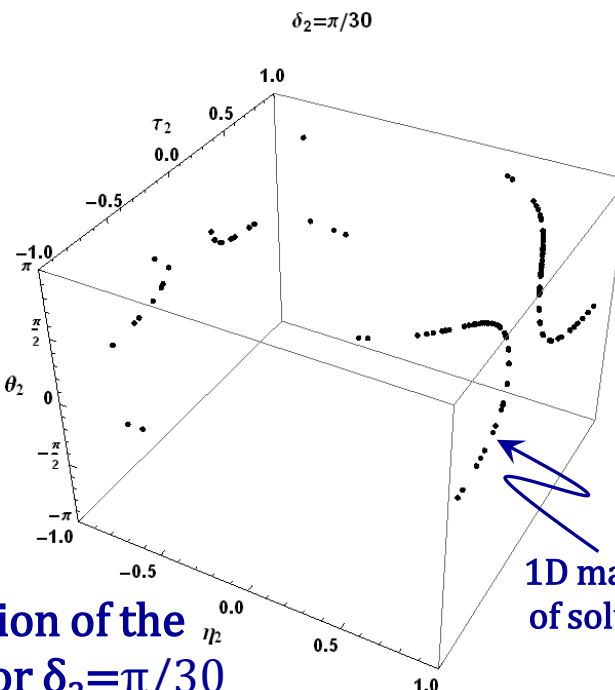
$$t_2^* = \sqrt{2(\sqrt{2} - 1)},$$

$$t_1^* = t_3^* = 1/(1 + 2\sqrt{2})$$



$$t_2^* = t_2^*(\eta_2, \tau_2, \theta_2)$$

$$= \sqrt{2(\sqrt{2} - 1)}$$



1D intersection of the
two surfaces for $\delta_2 = \pi/30$

1D manifold
of solutions

$$\delta_2 = \theta_{A2}(\eta_2, \tau_2, \theta_2)$$

$$= \pi/30$$